THE GEOLOGICAL SOCIETY OF AMERICA®

Detrital zircon provenance and transport pathways of Pleistocene-Holocene eolian sediment in the Pampean Plains, Argentina

Austin Bruner[1,2], Andrew L. Leier[3], David L. Barbeau, Jr.[3], Alex Pullen[1,†], Mary Kate Fidler[1], and Blake Stubbins[3]
[1]*Department of Environmental Engineering and Earth Sciences, Clemson University, Clemson, South Carolina 29634, USA*
[2]*Department of Geology, University of Kansas, Lawrence, Kansas 66045, USA*
[3]*School of the Earth, Ocean and Environment, University of South Carolina, Columbia, South Carolina 29208, USA*

ABSTRACT

The Pampas of Argentina contain a broad distribution of Pleistocene to Holocene loessic sediments and eolian dune deposits. Models describing the sediment provenance of this eolian system have, at times, conflicted. We address the provenance of these deposits through U-Pb detrital-zircon geochronology. Our results indicate broad similarity in age distributions between samples, with a dominant Permian-Triassic mode, and widespread but lesser Cenozoic, Devonian-Mississippian, Ediacaran-Cambrian, and Mesoproterozoic modes. These data are inconsistent with a large contribution of detritus from Patagonia as previously suggested. These data are consistent with very limited contribution of first cycle volcanogenic zircon to the Pampean eolian system, but abundances of older Neogene zircon indicate proto-sources in the Andes. The ríos Desaguadero, Colorado, and Negro contain populations that were likely within the dust production pathways of most of the loess, paleosol, and eolian dune deposits, but the derivation of the zircon ages in these sediments cannot be explained solely by these river systems. One statistical outlier, a loess sample from the Atlantic coast of the Pampa region, indicates quantitative similarity to the age spectra from the ríos Colorado and Negro, consistent with derivation from these subparallel rivers systems during subaerial exposure of the continental shelf under high global ice-volume. Another statistical outlier, a paleosol sample from the Río Paraná delta region, has zircon ages more closely associated with sediments in the Paraná region than in rivers south of the Pampa region. Collectively, these data point to the complexity of the Pampean eolian system and substantial spatial-temporal variation in this Pleistocene–Holocene eolian system.

INTRODUCTION

Dust plays a fundamental role in the Earth's climate by impacting nutrient cycling in the oceans (Jickells et al., 2005, Maher et al., 2010), affecting the radiative forcing budget of the planet (Sokolik et al., 2001; Huang et al., 2006; Kumar et al., 2011; Miller et al., 2014; Scanza et al., 2015), and perturbing snow-ice albedo (Hansen and Nazarenko, 2004; Painter et al., 2007). Dust lofted from southern South America is especially important for seawater chemistry in the South Atlantic and Southern Ocean's high-nutrient–low-chlorophyll regions with Fe-limited productivity (e.g., Church et al., 2000; Boyd and Law, 2001; Gaiero et al., 2003; Johnson et al., 2011; Moore et al., 2013; Paparazzo et al., 2018). By modulating Fe-delivery and bioproductivity in these regions throughout the Pleistocene (e.g., Martínez-Garcia et al., 2011; Anderson et al., 2014; Albani et al., 2016), dust from southern South America likely affected atmospheric CO_2 concentrations (Martin et al., 1990; de Baar et al., 1995; Ridgwell and Watson, 2002; Bopp et al., 2003; Abelmann et al., 2006).

Understanding South American dust production during the late Pleistocene is not as simple as examining modern dust activity and extrapolating into the geologic past. Dust fluxes during late Pleistocene cold periods were at least four times higher compared to interglacial periods (Martínez-Garcia et al., 2011; Shoenfelt et al., 2018), and were driven by different wind patterns (e.g., Toggweiler and Russell, 2008; Anderson et al., 2009; Boex et al., 2013). Bulk geochemical analysis of dust archived in the Antarctic Ice Sheet has been largely tied to proto-sources in Patagonia and the Altiplano-Puna Plateau (Gaiero, 2007; Gaiero et al., 2013; Gili et al., 2016) with some contributions from Australian deserts (Revel-Rolland et al., 2006). Although important for reconstructing original source areas, this bulk geochemical approach largely ignores changes in surficial conditions (precipitation, wind characteristics, vegetation) when characterizing potential source areas of dust during the Pleistocene, with some exceptions (e.g., Grousset et al., 1992; Gili et al., 2017; Delmonte et al., 2017). In addition to growth of the Patagonian Ice Sheet, surficial conditions during glacial periods stimulated large dust-generating provinces in the Pampean and Chaco plains (Sayago et al., 2001; Zárate, 2003). Without comprehensive reconstructions of dust production pathways (i.e., transfer from proto-sources through intermediate sources to its final deposition) the climate forcings of dust production remain obscured.

Equatorward shifts in the mean positions of synoptic-level winds in both hemispheres during Pleistocene glacial periods (e.g., Toggweiler and Russell, 2008; Vanneste et al., 2015; Abell et al., 2021) implies a northward migration of Southern Hemisphere westerly winds, as well as secular variations in effective precipitation, vegetation, stream- and lake-levels, and ice-volumes (Kohfeld et al., 2013; Berman et al., 2016; Martini et al., 2017). Such variations are known to have changed eolian activity in South America, which was suppressed during warmer periods like the Holocene (e.g., Kemp et al., 2004; Zárate et al., 2009; Forman et al., 2014; Tripaldi and Forman, 2016).

Loess, predominantly composed of silt-sized particles, exists in the natural continuum of eolian entrainment, transport, and deposition (Richthofen, 1882; Obruchev, 1911, 1945). Glacial loess and desert loess models have been put forth to describe the processes by which silt-sized particles are produced from parent rock materials (Tsoar and Pye, 1987; Smalley, 1995; Pye, 1995, Muhs, 2007). The former produces silt-sized particles through mostly glacial grinding, whereas desert loess models invoke a variety of non-glacial processes (e.g., eolian abrasion and impacts). Importantly, dust production pathways can include fluvial comminution and transport

Alex Pullen https://orcid.org/0000-0002-5583-5844
[†]Corresponding author: apullen@clemson.edu.

 https://doi.org/10.1130/B36267.1; 6 figures; 1 supplemental file.

(e.g., Lyell, 1834). Genetic links between rivers and loess deposits in subtropical to temperate climates with close spatial proximity to river systems have been well established (e.g., Mississippi River in North America: Russell, 1944; Krinitzsky and Turnbull, 1967; Grimley, 2000; Bettis et al., 2003; Crouvi et al., 2008; Smalley et al., 2009; Stevens et al., 2013; Nie et al., 2015); however, this thesis has been less widely applied to the majority of loess sequences.

The Pleistocene-Holocene dust production system of southern South America remains obscure, in terms of both the location of proto-source areas and the transport pathways (Zárate, 2007). Without this knowledge, we have few constraints for verifying paleoclimate models of the region. Like the loess units, the provenance of the eolian sand is also poorly constrained. Together, the loess and eolian sand deposits in central Argentina represent some of the largest eolian deposits on the continent. To better understand the continuum of eolian sediment production pathways of late Pleistocene-Holocene sediments exposed in central Argentina, we collected $N = 17$ samples of river, eolian dune, loess, and paleosol sediments reporting $n = 3744$ new detrital zircon U-Pb ages.

GEOLOGICAL SETTING

The Pampa Plains, or simply Pampas, consists of extensive plains with minimal topography located in central Argentina (Fig. 1). Boundaries between the Pampas and surrounding regions are transitional and their definitions commonly differ between individuals (e.g., Clapperton, 1993; Zárate and Tripaldi, 2012); however, the general dimensions and characteristics of the region are consistent. To the north, the Pampas grade into the Chaco Plain of northern Argentina and Bolivia, with the Río Paraná forming a northeastern boundary and the Sierras Pampeanas forming a northwestern topographic margin. To the west, the Pampas extend largely to the foothills of the Andes, although many place the boundary at the Río Desaguadero system and refer to the land located west of this river and east of the Andes as the Andean Piedmont. The Río Colorado represents the southern boundary of the Pampas, south of which lies the Northern Patagonian Plateau. All of these rivers include tributaries that emanate from the Andes to the west; however, there are discernable differences in sedimentary petrography (Garzanti et al., 2021a). The Pampas extend more or less continuously to the southern Atlantic Ocean in the east (Fig. 1).

The modern climate of the Pampas is humid to subhumid in the east, but becomes progressively drier to the west and southwest; precipitation levels decrease from >800 mm/yr in the east to the <500 mm/yr in the west (Clapperton, 1993; Prieto, 1996; Garreaud et al., 2009; Iriondo et al., 2009; Aliaga et al., 2017). This pattern is largely a function of the South Atlantic high-pressure system, which brings humid and

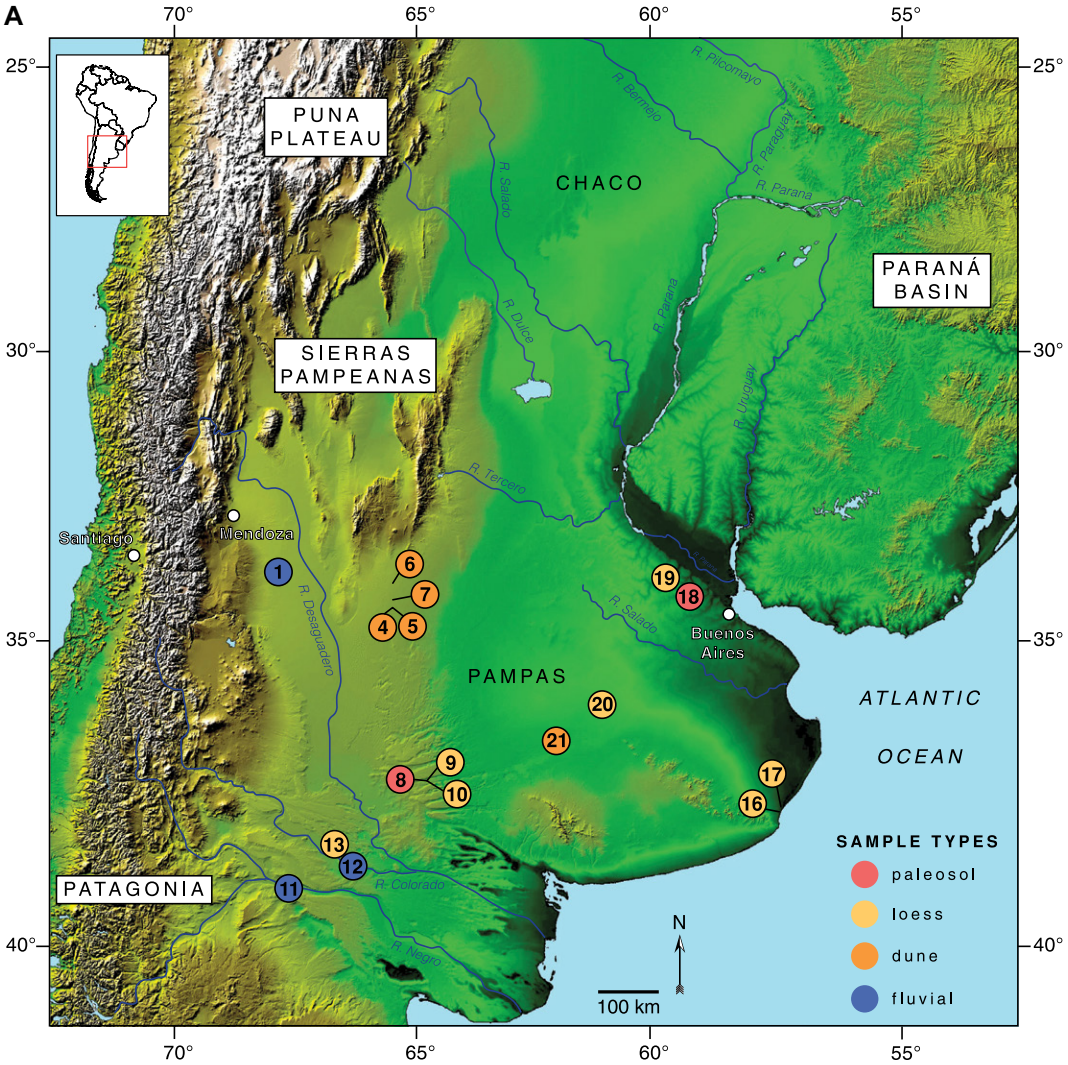

Figure 1. (A) Distribution of samples and sample types in southern central South America. All samples contain the prefix "19AR," which are referred to in text. (B) Simplified geologic map of the region, with sample locations shown, modified from the Gómez et al. (2019b). Cenozoic sedimentary rocks refer to units of Miocene-age and older. ACftb—Agrio-Chos Mal-Malargüe fold-thrust belt.

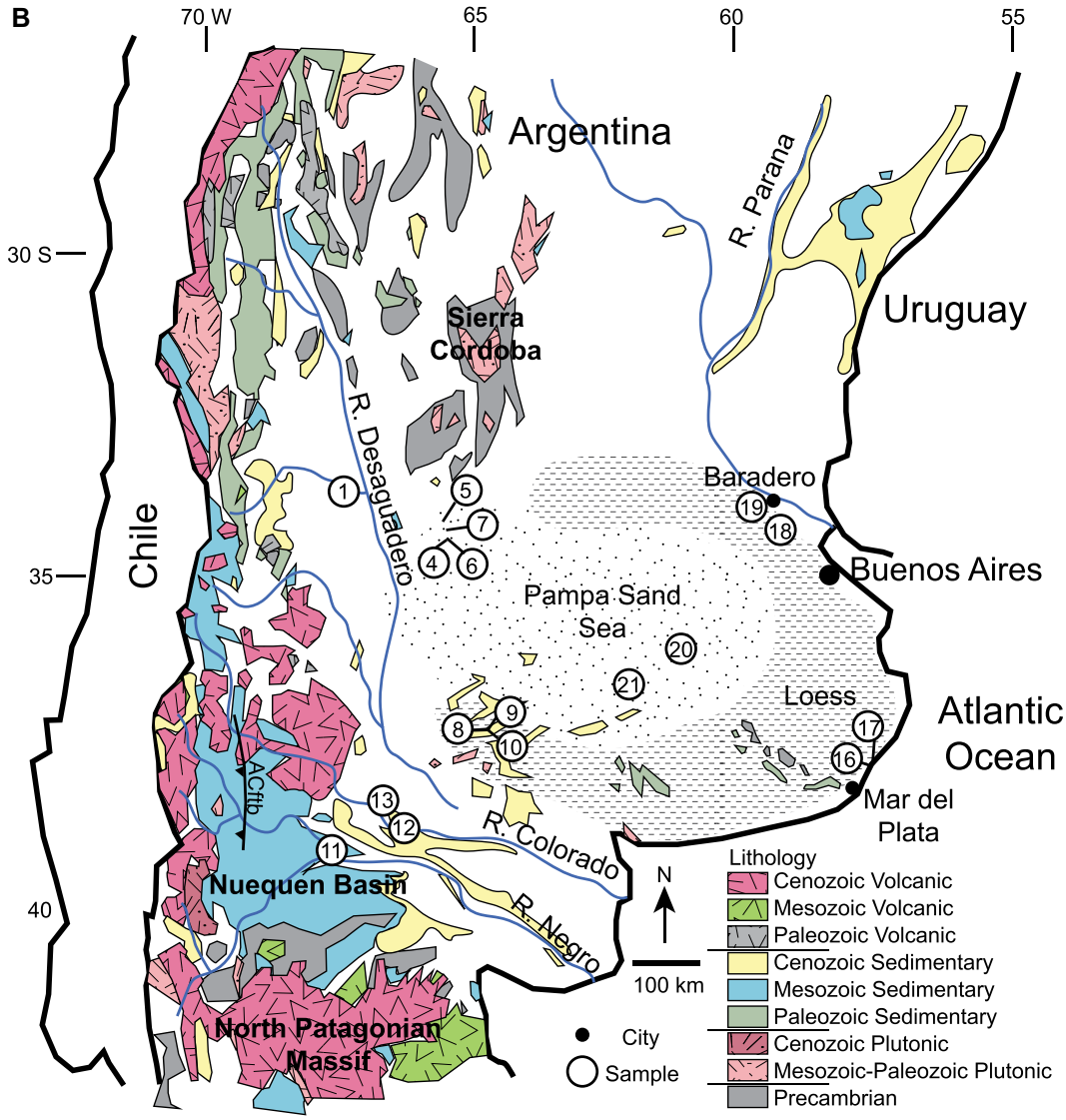

Figure 1. (***Continued***)

warm air across the region via northeasterly winds (Aliaga et al., 2017). However, there is ample evidence that the climatic conditions observed today were different during past cold periods. Most data suggests that during glacial episodes, climatic belts in the high latitudes of South America shifted northward, bringing stronger westerly winds and drier conditions to the Pampas (e.g., Iriondo, 1999; Rabassa et al., 2005; Wainer et al., 2005; Berman et al., 2016). Climate at the regional-scale also changed. Unlike modern wind patterns, eolian landforms from the Last Glacial Maximum record an anticlockwise wind pattern in the Pampas and central Argentina during this time (Iriondo and García, 1993). This, combined with katabatic winds from icefields in Patagonia would have produced strong ~southwesterly winds across much of the Pampas (Iriondo, 1997). Although the Pampas were drier, discharge increased for rivers emanating from the Andes, like the Río Desaguadero, due to higher precipitation and/or glacially sourced flow (Iriondo, 1997).

The Pampas contain large volumes of wind-blown sediment with both active and relict eolian dunes as well as extensive loess and loessoid deposits (Teruggi, 1957; Clapperton, 1993; Zárate and Blasi, 1993; Zárate, 2003; Tripaldi et al., 2011; Zárate and Tripaldi, 2012). The core of the wind-blown deposits in the Pampas is called the Pampa Sand Sea (Iriondo, 1997), a ~$3*10^5$ km^2 region of vegetation-stabilized eolian sand (Tripaldi et al., 2013). Dune morphology varies, but blowout, parabolic, and linear dunes represent the most common style (Zárate and Tripaldi, 2012; Tripaldi et al., 2018). Despite the aerial continuity of the Pampa Sand Sea, recent investigations suggest the deposits themselves are heterogeneous in nature and composition and often influenced by their proximity to sediment source areas, local and regional topography, and regional wind patterns (Zárate and Tripaldi, 2012). Loess deposits up to 30 m thick ring the southern, eastern, and northern border of the Pampa Sand Sea and are composed of loess and pedogenically altered loess horizons (Clapperton, 1993; Iriondo, 1997; Zárate, 2003). The loess consists of clay, silt, and very fine-grained sand composed of quartz, plagioclase, pyroclastic material, and volcanic glass (Teruggi, 1957; González Bonorino, 1965; Clapperton, 1993; Imbellone and Teruggi, 1993).

Loess and eolian sand in central Argentina are attributed to several possible sediment source areas. During past glacial periods, river and floodplain sediment are hypothesized to have been entrained by south-southwesterly winds and deposited in the Pampa Sand Sea and loessoid belt (Iriondo, 1990; Iriondo 1997; Kröhling, 1999). South-southwesterly winds may have

also entrained sediment from the Río Colorado and Río Negro, which flow along the southern border of the Pampas (Zárate and Blasi, 1993). This south-to-north hypothesis is supported by detrital zircon ages from Holocene eolian samples in the westermost Pampas (Capaldi et al., 2019). Rare earth element and Sm-Nd data from the loess support this hypothesis, suggesting a northern Patagonian sediment source with additional contributions from other regions (Smith et al., 2003). The central Andes may have also contributed to loess in the Pampas. This area has generated recent dust plumes (Milana and Kröhling, 2017) and contains evidence of long-term (m.y.) wind erosion (McMillan and Schoenbohm, 2020). Volcanic sediment has long been recognized as a source for loess in central Argentina (Teruggi, 1957), and certain areas contain evidence of local sediment sources (González Bonorino, 1965).

METHODS

We collected samples of loess, fluvial sand, eolian sand, and paleosols from across the Argentine Pampas and surrounding areas (Fig. 1). Age constraints are not available for all of the samples, but based on previous work from similar or proximal sediments (Kemp et al., 2006; Kruck et al., 2011; Tripaldi and Forman, 2016) the age of the samples range from modern to ca. 110 ka in age, with the majority being <70 ka in age. One exception to this is the paleosol sample 19AR08, whose age is unknown. Detailed descriptions of the samples, their age constraints and their sampling locations can be found in the Supplemental Material[1].

Detrital zircon crystals were separated from ~5 kg of sample. Indurated samples were disaggregated using a hand crusher, and all samples were passed through 600 μm disposable nylon sieve screen. To maximize zircon recovery from clay-rich samples and to minimize grain-size age biases from hydraulic sorting (e.g., Sláma and Košler, 2012; Ibañez-Mejia et al., 2018), zircon fractions were isolated using ultrasonic disruption following an approach modified from Hoke et al. (2014)—the only two modifications were stirring samples from above rather than below so larger sample volumes could be separated and using an ultrasonic tank for more evenly distributed ultrasonic wave energy and cavitation rather than relying on an ultrasonic probe. After ultrasonic separation, zircon crystals were separated in a heavy liquid and with a Frantz barrier field isodynamic magnetic separator.

The detrital zircon crystals were dated using an Element 2 single-collector inductively-coupled plasma–mass spectrometer coupled to a Photon Machines 193 nm excimer laser in the Center for Elemental Mass Spectrometry at the University of South Carolina, Columbia, following the methodologies of Pullen et al. (2018). Elemental- and mass-fractionation, instrument drift, and down-pit fractionation were corrected using a suite of reference materials mounted with the sample zircon in 2.5 cm epoxy ring forms. Laser spot size used for analyses was 25 micron. Corrections were made using an in-house Excel based data program (AgeCalc; Gehrels et al., 2006). The suite of reference materials included Sri Lanka, FC-1, and R33 (Paces and Miller, 1993; Black et al., 2004; Gehrels et al., 2008; Mattinson, 2010). This approach yielded the correct age of the monitoring reference material within ±2% or less (at 1σ). Single-grain U-Pb ages were not considered further if $^{206}Pb/^{238}U$ uncertainty was >10% (1σ), $^{206}Pb/^{207}Pb$ uncertainty was >10% (1σ), if age discordance was >30%, or reverse discordance was >5% for grains older than 600 Ma. The discordance on ages <600 Ma was not considered because of the challenges of accurately measuring $^{206}Pb/^{207}Pb$ in young crystals. Plots and interpretations use the $^{206}Pb/^{238}U$ age if the $^{206}Pb/^{238}U$ age is <1000 Ma, and the $^{206}Pb/^{207}Pb$ age if the $^{206}Pb/^{238}U$ age is ≥1000 Ma.

RESULTS

In Figures 2 and 3, we present the U-Pb age distributions of detrital zircons from $N = 17$ sediment samples collected from fluvial, paleosol, and eolian deposits of central Argentina. With the exception of loessoid sample 19AR19 collected from a bluff of the lower Río Paraná (Fig. 1), there are many similarities in the distribution of age populations between samples (Figs. 2 and 3). When the samples are combined into a single composite plot (bottom of Fig. 2), eight prominent age populations emerge, with peaks, from largest to smallest, at: [1] Permian-Triassic (25% of all dated grains, ranging from 21% to 36% of grains of each sample, excluding 19AR19); [2] Devonian-Mississippian (13%; range: 8%–28%); [3] Cenozoic (11%; range: 3%–18%); [4] Ediacaran-Cambrian (11%; range: 4%–16% but composing 43% of 19AR19); [5] late Mesoproterozoic (8%; range 3%–18%); [6] Jurassic (8%; range: 4%–18%); [7] Cretaceous (8%; range 2%–17%), and [8] Ordovician (8%, range: 4%–12%). The remaining zircons largely form small Neoproterozoic and Paleoproterozoic populations, or occur between significant age modes.

Figure 2. Detrital zircon U-Pb age distributions of fluvial and eolian units from central Argentina. Kernel density estimates are filled polygons constructed with a Epanechnikov kernel with a 15 m.y. bandwidth, are color-coded to their depositional system and area-normalized between samples. Probability density plots are depicted by red curves and are area-normalized except where indicated by break-in-scale hash marks for some Cenozoic populations. Plot at bottom depicts the collective distribution of zircon ages from all 17 samples, revealing the prominent age modes that are present in most samples, shown by gray polygons. Note that 67 grains have ages older than 2 Ga and, therefore, do not appear in the plot.

Of the largest populations, the Permian-Triassic (present in all 17 samples, prominent in all but 19AR19); Jurassic (present in all but 19AR19; prominent in eight samples); and Cretaceous (present in all but 19AR07; prominent in four samples) modes are the most ubiquitous (Figs. 2 and 3). Although less sizable, the Devonian-Mississippian, Ordovician, and late Mesoproterozoic populations are comparably widespread across the suite of samples. Whereas there are many Cenozoic zircon age populations, the largest individual modes are Quaternary in age (Fig. 3).

Despite great similarities of zircon age distributions between our samples, some aspects of our results warrant particular mention. We note that with the exception of 19AR19 and 19AR17, all eolian (loess, loessoid, and dune sand) samples have reasonably similar presence-absence and population abundance relationships. Both 19AR19 and 19AR17 differ from other eolian samples in their scarcity of Neogene zircons. Sample 19AR19 differs from other samples in the dominance of the Ediacaran-Cambrian age mode and the absence or minor abundances of most other age modes that are otherwise present throughout our samples. Sample 19AR17 differs from other samples by its dominance of the Cretaceous age mode. Finally, we note the relative paucity of Neogene age zircons in all of our fluvial and paleosol samples in contrast to the loess, loessoid, and dune samples, excluding the aforementioned 19AR19 and 19AR17.

PROVENANCE OF ZIRCON AGE MODES

Zircon crystals in our samples with ages of 0–65 Ma are interpreted as originally derived

[1]Supplemental Material. Table S1: U-Pb geochronologic analyses. Please visit https://doi.org/10.1130/GSAB.S.19420217 to access the supplemental material, and contact editing@geosociety.org with any questions.

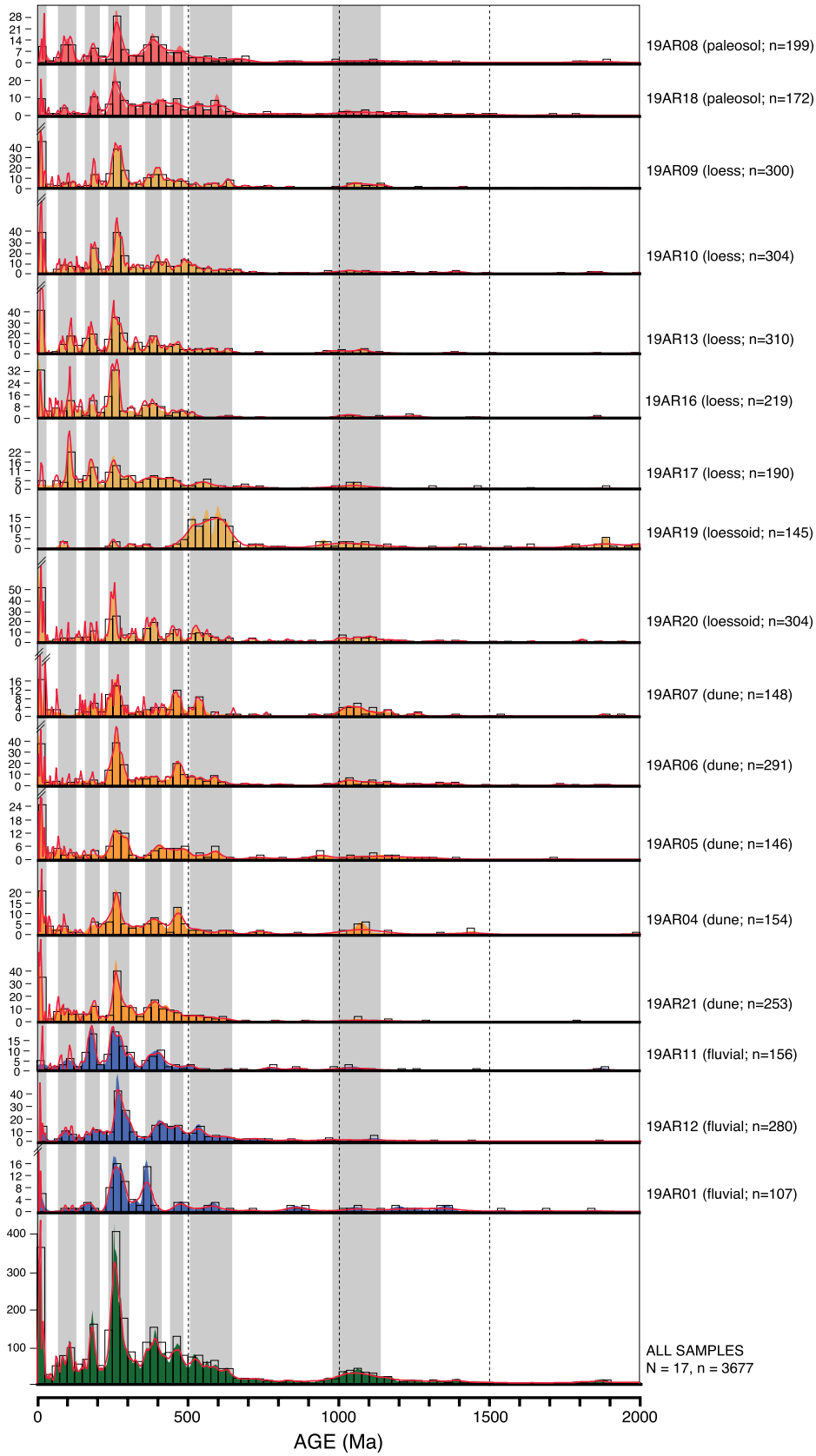

from subduction-related magmatic arc rocks in the Andes, which are well-exposed throughout the Andean Cordillera (e.g., Balgord, 2017; Capaldi et al., 2017; Gomez et al., 2019). We interpret the 65–145 Ma zircons that are significant in many of our samples as also largely being derived from the Andean magmatic arc, likely from more southern latitudes of the study area where older batholithic rocks are exposed; Cretaceous magmatic arc rocks are restricted to the west side of the continental divide north of ~42°S (Gomez et al., 2019). Alternatively, some Cretaceous zircons may have been derived from igneous rocks in the Paraná Basin (Fig. 1) to the east of the study area, although most of the appropriately aged units have basaltic lithologies that are unlikely to be zircon-fertile. We interpret the 150–200 Ma age mode (i.e., Jurassic) prominent in many of our eolian samples as being derived from the Chon Aike silicic Large Igneous Province associated with the breakup of Gondwana (Pankhurst et al., 1998). Whereas these rocks are more widely exposed in Patagonia, there are significant exposures at the latitudes of the study area in the forearc of the Andes, but these outcrops are west of the present continental divide (Gomez et al., 2019). Therefore, it is likely that Jurassic zircons in our sample were originally derived from the North Patagonian Massif to the south of the study area. Notably, there is a prominent Jurassic age mode in all of the reported modern samples from the greater Río Colorado and Río Negro systems (average 15%, range 5%–22%, $N = 8$: our samples 19AR11 and 19AR12 and Pepper et al., 2016), and Chubut River (32%, $N = 1$: Pepper et al., 2016) in the southern part of the study area, yet there are no Jurassic zircons from samples of the Río Bermejo or Río Pilcomayo of the greater Paraná watershed to the north ($N = 4$: Pepper et al., 2016). The likely immediate source of these zircons is Jurassic and younger strata originally deposited in the Nuequén Basin and later exhumed in thrust sheets within the Agrio-Chos Mal fold-thrust belt (Fig. 1B; e.g., Ramos et al., 2004).

We interpret the large 240–280 Ma detrital-zircon age mode in all but one of our samples as being originally derived from the Permo-Triassic Choiyoi magmatic province that developed across a wide swath of south-central South America between northern Chile and northern Patagonia (Sato et al., 2015; Bastías-Mercado et al., 2020). Today, Choiyoi plutonic and volcanic rocks are widely exposed just west of the study area in the Andean Cordillera and in the North Patagonian Massif immediately south of

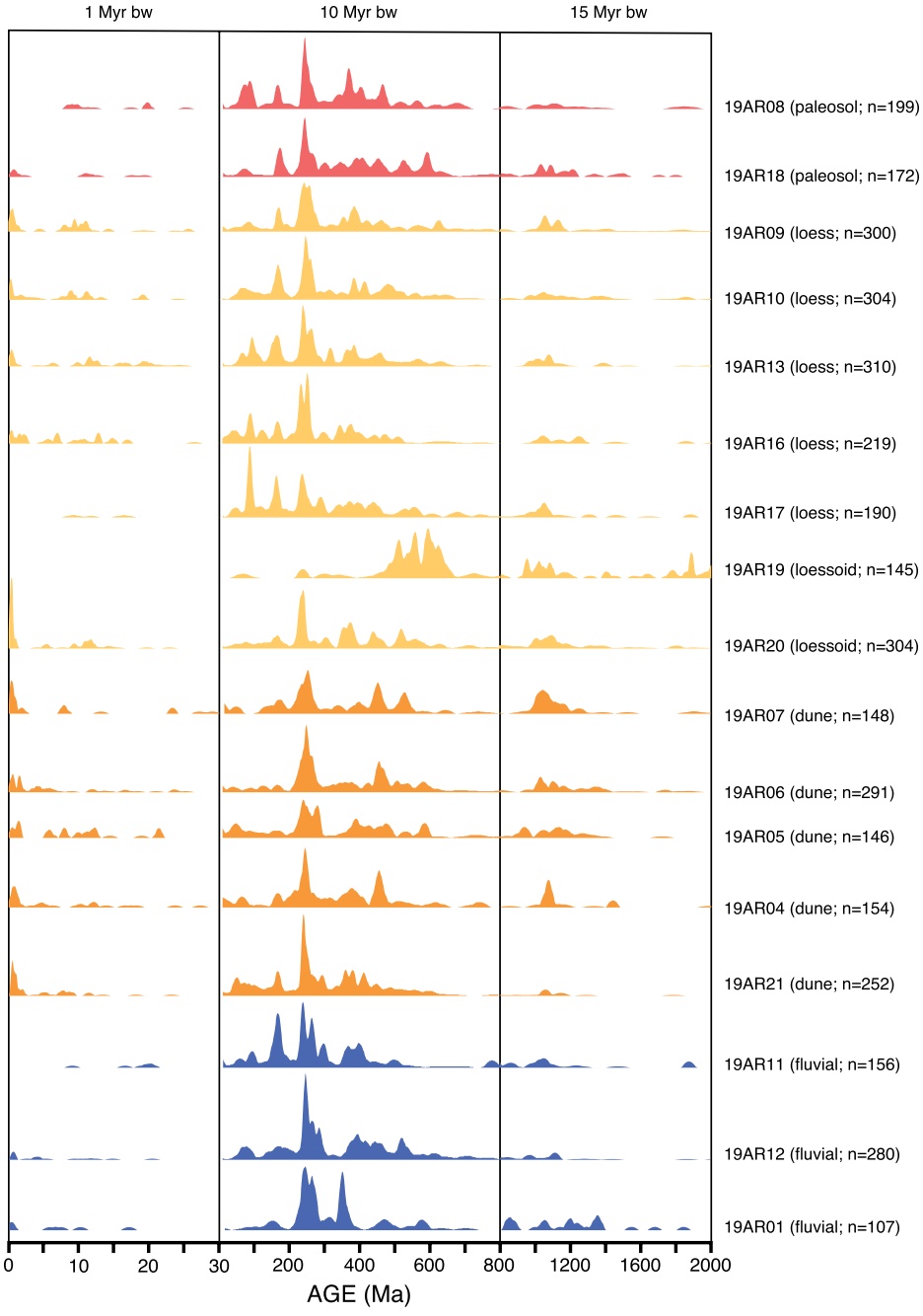

Figure 3. Age distribution of individual samples from central Argentina plotted using area-normalized Kernel density estimates with age segments of different Epanechnikov kernel bandwidths ("bw") and horizontal scales to best depict the true zircon age distribution of our individual samples. Note that 67 grains have ages older than 2 Ga and, therefore, do not appear in the plot.

the study area (e.g., Luppo et al., 2018; Gomez et al., 2019). Contemporaneous volcanic and volcaniclastic strata likely derived from the Choiyoi province outcrop broadly in the Paraná Basin east of the study area (Rocha-Campos et al., 2011). This age mode is also dominant in sedimentary rocks of the Nuequén Basin (e.g., Naipauer et al., 2015) and in low-grade early Mesozoic metasedimentary complexes exposed in the southern Chilean Andes (Hervé et al., 2003, Barbeau et al., 2009), although these rocks are primarily exposed west of the continental divide. Whereas this dominant and all but ubiquitous age mode indicates sediment derivation from south-central South America, the widespread nature of these source rocks precludes the use of the 240–280 Ma age mode as a diagnostic provenance tool at these latitudes. However, this age mode is the dominant component of modern fluvial deposits in the Río Colorado and Río Negro systems of the southern part of the study area, composing 28% of zircons sampled therein (range 15%–36%, $N = 8$: our samples 19AR11 and 19AR12 and Pepper et al., 2016). In contrast, this age mode is noticeably minor (1%–4%, $N = 4$) in samples collected from the Río Pilcomayo and Río Bermejo (Pepper et al., 2016) of the greater Paraná watershed in the northern and western part of the study area (Fig. 4).

We interpret the 280–360 Ma detrital zircon mode as being originally derived from a Carboniferous arc, which formed along the Gondwana margin (Mpodozis and Kay, 1992; Sato et al., 2015; Naipauer et al., 2015), and the 440–500 Ma detrital zircon population as derived from the Famatinian arc (Ramos, 2009). Ordovician batholithic plutons of the Famatinian arc are widely exposed in the central-western Sierras Pampeanas (e.g., Otamendi et al., 2020). Carboniferous plutons occur in the northwestern Sierras de Pampeanas and in the Sierras de Córdoba of the eastern Sierras Pampeanas (Morosini et al., 2017), and are interpreted to have intruded the Famatinian back-arc region following collision of the exotic Cuyania terrane, detachment of the subducted slab, and/or orogenic collapse (Otamendi et al., 2020).

We interpret zircons with ages between 500 and 700 Ma, which dominate sample 19AR19 and form minor components of our other samples, as being originally derived from plutonic rocks formed during the Brasiliano and Pampean orogenies as part of the large Pan-African tectonic event. Collectively, igneous rocks of this age surround the Río de la Plata craton that forms the basement to the Pampas and are today exposed in the eastern Sierras Pampeanas (e.g., Sierra Cordoba; Schwartz et al., 2008). In addition, metasedimentary units exposed in the eastern Sierras Pampeanas also contain zircons with ages of 500–700 Ma (Rapela et al., 2016). Widely exposed Ordovician sedimentary strata in the northern Argentine Precordillera contain a significant 500–700 Ma age mode (DeCelles et al., 2007; Augustsson et al., 2011; Enkelmann et al., 2014; Ramos et al., 2014; Thomas et al., 2015; Amidon et al., 2016) presumably derived from the underlying Pampean and Brasiliano plutons, and may have provided more direct sources of 550–700 Ma zircons to our other samples. This population is the dominant mode in modern samples from the Río Bermejo and Río Pilcomayo draining the Central Andes,

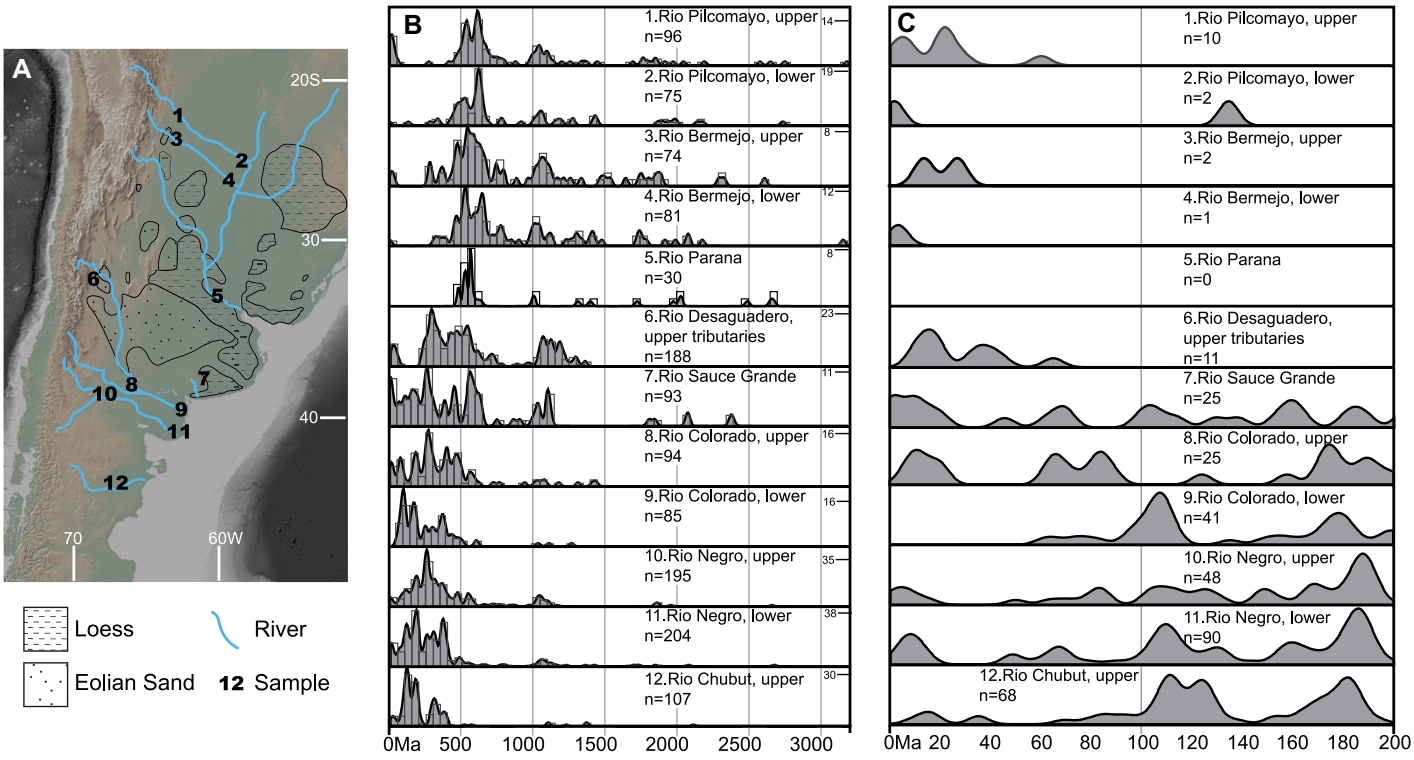

Figure 4. Existing detrital-zircon data from modern rivers in the Central and Southern Andes. (A) Digital elevation model image of southern South America with rivers, eolian deposits, and sample locations. (B and C) Detrital zircon data from modern rivers. (B) Zircon age distribution of samples for grains with ages between 0 and 3200 Ma. Kernel density estimates (KDE) and histogram are shown. (C) KDE results of detrital zircons with ages <200 Ma. Sources for data: 1–4 and 7–12 Pepper et al. (2016; original samples: CA01, CA02, CA03, CA04, SA06, SA07, SA08, SA09, SA11, and SA12 combined, SA15); 5 Rino et al. (2008; original samples: Para); 6 Capaldi et al. (2017; original combined samples RBMJ01 and RSJN03).

composing between 31% and 47% of zircons in those samples ($N = 4$, Pepper et al., 2016). This age mode is considerably smaller in modern samples from the greater Río Colorado and Río Negro systems (average 6%, range 1%–11%, $N = 8$, our samples 19AR11 and 19AR12 and Pepper et al., 2016), and Río Chubut (1%, $N = 1$: Pepper et al., 2016) in the southern part of the study area (Fig. 4).

We interpret the 900–1200 Ma zircon age mode that forms a small but consistent population in all of our samples as being originally derived from rocks associated with the Sunsas Orogeny (Bahlburg et al., 2009), which is equivalent in age to the Grenville Orogeny of North America (Tollo et al., 2004). The Laurentian Cuyania terrane in the western part of the study area contains Sunsas-age zircons (Ramos, 2009). These rocks are dominant components of the Pie de Palo and Valle Fértil ranges of the western Sierras Pampeanas, but this age mode is also the dominant component of the detrital zircons in Ordovician siliciclastic rocks in the Argentine Precordillera (Thomas et al., 2015). This Sunsas-age mode forms a significant component of modern samples from the Río Bermejo and Río Pilcomayo (Fig. 4), constituting between 15% and 18% of zircons in those samples ($N = 4$, Pepper et al., 2016). This age mode is considerably smaller in modern samples from the greater Río Colorado and Río Negro systems (average 6%, range 2%–10%, $N = 8$: our samples 19AR11 and 19AR12 and Pepper et al., 2016), and Chubut River (4%, $N = 1$: Pepper et al., 2016) in the southern part of the study area.

DISCUSSION

Input from First Cycle Volcanogenic Sources

Our U-Pb detrital zircon data suggest the possibility of first cycle volcanogenic zircon crystals within the loess, paleosol, and eolian dune samples. However, the number of possible first cycle zircons is limited. This is ostensibly at odds with long-held assertions of ash fall as an important source of detritus for the loessic sediments (e.g., Teruggi, 1957). The depositional age (i.e., most recent activity) of the eolian dune samples is taken to be less than 100 ka (see Supplemental Material for depositional ages); most recent activity is more likely 4–22 ka (Tripaldi and Forman, 2007, 2016). Using a depositional age of <100 ka for the eolian dunes and comparing this to the U-Pb ages of the detrital zircons, the percentage of ages ≤100 ka ranges from 0.0%–1.0% for the eolian dune samples reported here. Depositional ages have been determined for some, but not all of the loess and paleosol samples (see Supplemental Material; e.g., Kruck et al., 2011). Of the loess samples, detrital zircon crystals ≤100 ka were not identified in $N = 3$ samples. This could point to a "true" absence of <100 ka crystals in those samples or undersampling such that a low probability age mode was not identified. Where grains with ages ≤100 ka were identified, the populations were in the range of 0.33%–0.96% (when uncertainties on the age were considered). Zircon crystals ≤100 ka were not identified in either of the paleosol samples. Collectively, these statistical observations are interpreted to mean that the contribution of first cycle volcanogenic zircon crystals to loess, paleosol, and eolian dune samples was minimal. This does not preclude the input of recycled volcanic material, which is suggested by altered volcanic glass present in some loess deposits (Teruggi, 1957).

The absence of first cycle volcanigenic zircon crystals in eolian dune, loess, and paleosols samples from central Argentina is surprising given the proximity to the Andean volcanic arc; however, it is consistent with the regional geological history. As with other cordilleran-style orogens, magmatism and volcanism in the Andes is tied to the nature of subduction along the western margin of the continent (e.g., Ramos and Folguera, 2009). Flat slab subduction in the latitudes of central Argentina, notably in the Pampean and Payenian slabs, have resulted in diminished magmatism and volcanism, thus reducing the potential source of syndepositional volcanic zircons (Ramos 2009; Capaldi et al., 2021). Moreover, the recent (<1 Ma) volcanism that has occurred in these latitudes has been mafic in composition (Ramos and Folguera, 2011), and serve as zircon-poor source rocks. Thus the apparent incongruity between the Andean volcanic arc and the lack of first cycle volcanic zircons in the eolian deposits of the Pampas is reasonable and even predictable given the subduction and volcanic histories in this portion of the Andes.

Most of the loess and eolian dune samples yielded a higher relative proportion of <30 Ma crystals than the fluvial samples. The percentage of Neogene ages in the fluvial samples were in the range of <3.2%–5.6%. The percentage of those ages for the eolian dune samples were in the range of 9.9%–19.1%, whereas the loess samples yielded percentages of 0.0% (19AR19), 2.6% (19AR17), 12.4% (19AR10), 12.7% (19AR13), 14.2% (19AR09), and 15.0% (19AR16). Recognizing that 19AR19 and 19AR17 are outliers for reasons discussed below, the other three loess samples have Neogene age populations similar to the range observed in the eolian dune samples. These observations are interpreted to mean that the Miocene and younger volcanic rocks in the Andean Cordillera made a notable contribution of detritus to the eolian sediments of the Pampas, specifically the eolian dunes and loess deposits reported here (Fig. 4). Additionally, we interpret the likely statistically significant difference between the fluvial samples and loess and dune deposits suggests that wind deflation of the floodplains of these river systems alone could not be used to explain the detrital zircon ages spectra of the loess and eolian dune units.

Rivers as Sediment Delivery Systems

Our river samples show both similarities and dissimilarities to previous published data from river, bedrock, and sediment samples (Fig. 5), noting that some differences may be an artifact of sampling localities. Additionally, fractionation of sediment during transport (e.g., Ibañez-Mejia et al., 2018, undersampling of detrital zircon ages from samples (e.g., Pullen et al., 2014), and/or the addition of sediment between the sample localities of the respective rivers could explain the observed differences. Not surprisingly, our Río Negro sample (19AR12) sampled near the confluence of the Río Limay and Río Neuquén plot in proximity to one another in multidimensional scaling (MDS) space (Fig. 5B).

The provenance of windblown material in the Pampas is ultimately tied to the rocks of the Andean orogen (Zárate and Blasi, 1993; Morrás, 1997). However, two important questions arise: (1) from where in the Andes, specifically, is the sediment generated? and (2) what was the transport pathway of eolian sediments deposited in the Pampas? By transport "pathway" we mean the route and mechanism (e.g., eolian) by which sediments are transported from source area to depositional basin. Existing hypotheses of sediment provenance include the southern Puna Plateau, the Andes of Central Argentina, the northernmost Patagonian Andes and local sources, whereas mechanisms of transport are largely attributed to either a combination of fluvial and eolian transport or purely eolian transport (Teruggi, 1957; Gonzales-Bonorino, 1965; Iriondo, 1990, 1997; Kröhling, 1999; Zárate and Blasi, 1993; Smith et al., 2003; Milana and Kröhling, 2017).

Floodplain deflation is a common process for supplying dust for loessic sediments in temperate climates or glacier-fringing environments (e.g., Muhs, 2007, 2013; Smalley et al., 2009). However, recently, in part through the advantage of U-Pb detrital zircon dating as a provenance discrimination tool, desert fringing loess provenances have, in some instances, been shown to have genetic relationships with rivers through floodplain deflation (Muhs, 2013; Nie

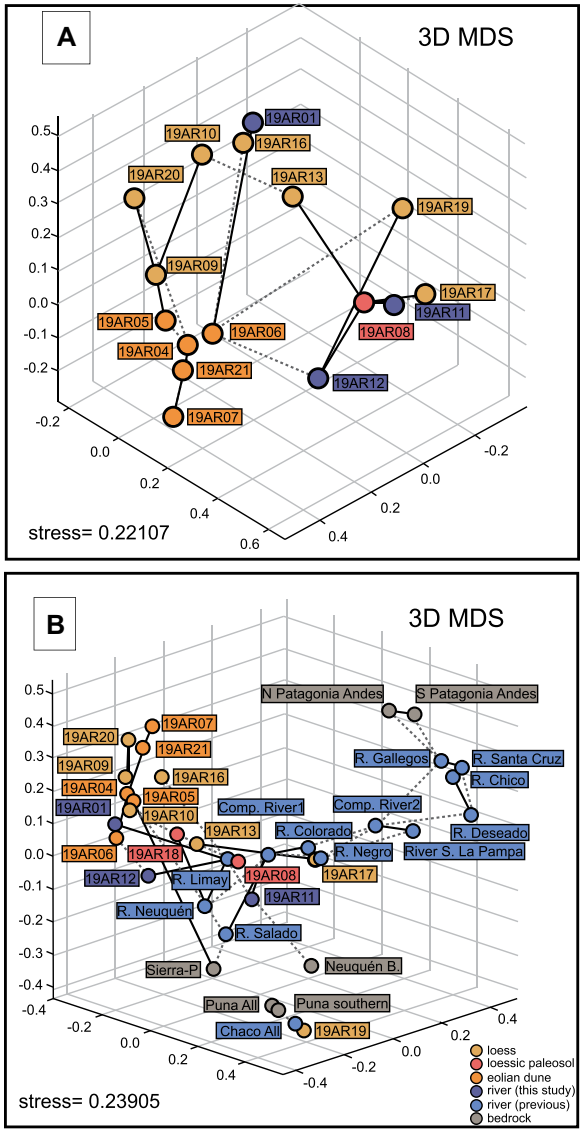

Figure 5. Three-dimensional multidimensional scaling (3-D MDS) plots of detrital-zircon age data. (A) Samples reported in this study of central Argentina. (B) Samples reported in this study plotted with comparison data from the Sierras Pampeanas (Sierra-P; Adams et al., 2011; Fosdick et al., 2015, 2017; Capaldi et al., 2017; Reat and Fosdick, 2018); southern Puna Plateau (Zhou et al., 2016, 2017); central Puna Plateau (included in "Puna All"; Siks and Horton, 2011; DeCelles et al., 2007; Streit et al., 2017; Henríquez et al., 2019, 2020); Chaco Plain (McGlue et al., 2016; Pepper et al., 2016); southern South American rivers (Pepper et al., 2016); N. Patagonia Andes (Encinas et al., 2014); S. Patagonia Andes (Leonard et al., 2020); and Neuquén Basin (Neuquén B.; Balgord, 2017). Compilation of rivers (Comp. River1: ríos Colorado, Negro, Limay, Salado; Comp. River2: ríos Colorado, Negro, Chubut). River S. La Pampa: includes all rivers south of La Pampa region from Pepper et al. (2016).

et al., 2015). This concept applies to the Negev Desert loess with the Nile River and delta, and the Chinese Loess Plateau with the upper Yellow River (e.g., Enzel et al., 2008; Amit et al., 2011; Bird et al., 2015). Similarities between the fluvial samples reported here and the eolian samples suggest floodplain deflation may have provided an important portion of the detritus to the eolian system.

The detrital zircon age populations for most of the eolian samples reported here—excluding 19AR17 and 19AR19 which will be discussed in more detail below—plot in proximity to the Río Desaguadero sample (19AR01) in MDS space (Fig. 5B), and close to our samples from the Río Colorado (19AR12) and Río Negro (19AR11) in central Argentina. As noted above, deflation of the rivers' floodplains cannot alone explain most of the age spectra from the eolian samples because of the dearth of Neogene zircons in the fluvial samples which were observed compared to the higher relative proportion in most of the eolian samples (Fig. 3). We tentatively interpret these data to indicate that a large portion of silt and larger detritus of the Pampean Sand Sea and loessic sediments the central Pampa plain was deflated from the Río Desaguadero floodplain. A contribution from the Río Colorado and Río Negro cannot be excluded based on the data presented here. A comparison between the data for our eolian samples with extra-Andean Patagonia rivers and Patagonian bedrock samples does not support the notion that the Patagonian region supplied much sediment (of silt-size and larger) to the eolian system of the Pampa region.

Southern Pampean Loess and the Atlantic Continental Shelf

Changes in sea-level have dramatically affected sedimentation on the 170–475-km-wide continental shelf south and east of Buenos Aires Province, Argentina (Violante et al., 2014). During periods of high global ice volume in the Pleistocene, subaerial exposure of the continental shelf made the area a potential eolian sediment source (Zárate and Blasi, 1993). Sample 19AR17, a loess sample from near the city of Mar del Plata on the Argentine Atlantic coast, shows quantitative difference with the loess samples from the central Pampa region. In addition, in 3-D MDS space, it plots near the Río Colorado and Río Negro samples of Pepper et al. (2016) and our Río Negro sample (19AR11). The dissimilarities are different from 19AR16, also from the Atlantic margin near Mar del Plata, which plots closer to the central Pampa samples (e.g., 19AR09).

Falling sea-level implies a large marine regression on the Atlantic continental shelf and slope such that Río Colorado and Río Negro would flow across the shelf due south of the Pampa region during a low-stand (e.g., approximately Last Glacial Maximum) rather than terminate near their current deltas. Following the hypothesis of Zárate and Blasi (1993), sample 19AR17 is consistent with derivation from sediments supplied from the Río Colorado and Río Negro due south of the Pampa region during marine regression. If valid, this hypothesis would suggest that these sediments were largely carried by southerly to southwesterly winds. Interestingly, 19AR16 probably would not fit the same scenario. In the absences of depositional age control on 19AR16 and 19AR17, we speculate that they have different depositional ages; 19AR17 from a period with relatively low sea-level and 19AR16 with a period of higher sea-level when more of the shelf was submerged. That scenario would suggest that during periods of higher sea-level, dust delivered to the Mar del Plata region had more in common with the central Pampa loess and the Pampa Sand Sea. Such a course of events may indicate a change in the orientations of the winds or surficial changes allowing or suppressing dust generation at different times.

Alternatively, recent sediment provenance data demonstrate significant northward-directed longshore sediment transport occurs along the Argentine Atlantic coast. Today, the "Colorado littoral cell" transports sediment >700 km from the deltas of the ríos Colorado and Negro northward along the eastern coast of Argentina (Garzanti et al., 2021b). Similarities between the detrital zircon populations of the coastal loess sample 19AR17 and those of the ríos Colorado and Negro can be interpreted to reflect this longshore transport and subsequent reworking in eolian conditions, rather than entrainment from the exposed coastal shelf during sea-level lowstands (e.g., Zárate and Blasi, 1993). These two hypotheses are not mutually exclusive, and it is possible that both longshore transport and shelf deflation during lowstands are important sources of wind-blown sediment along coastal Argentina (eastern Pampas). Further sampling and a combination of additional detrital zircon and sedimentary provenance data will be required before this sediment distribution system can be completely delineated. Additional research is needed to better understand why some coastal loess deposits are more similar to the ríos Colorado and Negro (e.g., 19AR17) and others more similar to loess from the central Pampas (e.g., 19AR16).

Loess and the Río Paraná

Of the sediments collected and analyzed as part of this study, sample 19AR19 is a clear outlier (Figs. 2 and 4), containing zircon populations that differ from all other samples. Sample 19AR19 was collected from an exposure of loess near the town of Baradero, Argentina, located ~135 km northwest of Buenos Aires along the southern bank of the Río Paraná (Fig. 1). Collected from ~1 m below the cliff-forming surface, the sample has a depositional age between 14.4 ka and 27.8 ka (Kemp et al., 2006), which overlaps with deposition of sediment across much of the Pampa Sand Sea (Kruck et al., 2011). Unlike all other samples we collected, 19AR19 is characterized by a dominant population of zircons with Pan-African ages between ca. 500 and 700 Ma and relatively few grains with ages <500 Ma (Figs. 2 and 3). This is true even when compared to sample 19AR18, which was collected only 50 km to the south.

The unique detrital zircon signature of sample19AR19 is interpreted as a function of its proximity to the Río Paraná (Fig. 1). We do not want to overstate the importance of a single sample; however, it can be informative for understanding the provenance of loessoid deposits in other parts of South America, notably northeastern Argentina and Uruguay (Zárate 2003). The Río Paraná extends for nearly 5000 km and has a drainage basin of $2.5*10^5$ km^2 that includes both southern Brazil and the Eastern Cordillera of the Central Andes. Bedrock in the basin is highly variable but basement rocks consist primarily of Pan-African age units (Rino et al., 2008). Modern river sediments reflect this with dominant detrital zircon populations of Pan-African age (Fig. 3; Rino et al., 2008). Although the data are associated with a relatively small *n* (25), roughly 75% of detrital zircons in the Río Paraná have ages between 500 and 700 Ma. This population overlaps that found in the 19AR19 sample. At this point it is impossible to pinpoint the exact source of Pan-African age detrital zircons in the Río Paraná drainage basin; however we do note that this population is present in rocks in the Sierra Pampeanas (Rapela et al., 2016) and in rivers exiting the Andes in Bolivia and northwestern Argentina (Fig. 4; Pepper et al., 2016), which serve as tributaries to the Río Paraná. Sedimentary units exposed in the drainage basins of these rivers, which would serve as sediment sources, contain populations of Pan-African age detrital zircons (DeCelles et al., 2007; Amidon et al., 2016; Enkelmann et al., 2014).

The similarity between detrital zircon populations in 19AR19 and the Río Paraná as well as their spatial proximity suggests a genetic relationship. We posit that the Río Paraná represents the principal component of the sediment transport pathway responsible for depositing the loessoid units associated with the 19AR19 sample. In addition to transporting sediment down river, the Río Paraná deposits sediment along its length

in floodplain environments (e.g., Amsler et al., 2007). We interpret the loessoid unit associated with sample 19AR19 as having been reworked sediment originally deposited in the Río Paraná floodplain. These loessoid deposits appear to faithfully record the preponderance of Pan-African detrital zircons in the riverine sediments.

The detrital zircon signature in 19AR19 has two important ramifications for loess and loessoid deposits in Argentina and elsewhere in southern South America. The unique detrital zircon populations underscore previous investigators' findings that suggest the areally extensive loessoid deposits in central Argentina are not homogenous. Through various methods, previous researchers have noted that despite their similar appearance, not all central Argentine loess deposits are the same (e.g., Zárate and Tripaldi, 2012). Our results support this hypothesis, and suggest that, in the future, detrital zircon geochronology will be an effective method for discerning individual depocenters across the region.

The second implication pertains to the provenance of loess deposits elsewhere in South America. We attribute the spatially limited provenance signature of 19AR19 to regional wind patterns during deposition, most notably, the influence of southwesterly winds (e.g., Iriondo, 1997). Past conditions that were dominated by southwesterly winds means that windblown sediment deposited in the Pampas would have had southwestern sources. Sediment from the Río Paraná would not have contributed to deposits located upwind (southwest), except in areas immediately adjacent to the river, like the location of 19AR19. But how unique is the detrital zircon signature of 19AR19? For much of the windblown sediment in the Pampas, it appears to be relatively rare, but in other loessoid units we predict it is very common. The same southwesterly winds that controlled sediment delivery to the Pampas would have also entrained sediment along the Río Paraná and deposited it downwind (northeast). Other loessoid deposits in South America include those in Uruguay, Paraguay, and southernmost Brazil (Panario and Gutiérrez, 1999; Iriondo and Kröhling, 2007). Given southwesterly winds, these areas would be located downwind of the Río Paraná and are therefore the most likely depocenters for windblown sediment from the Río Paraná system. We speculate that loessoid deposits in these regions are dominated by detrital zircons with ages similar to those observed in the Río Paraná and distinct from loess and loessoid deposits in the Pampas.

SUMMARY

The data presented here provide new insight into the origin and transport pathways of windblown sediment in central Argentina and can be used to formulate new hypotheses which will require further testing. Below we note three insights gleaned from our new data which may provide guidance to better understand the Pampean eolian system in the future.

(1) The number of zircons <100 ka observed in Pampean eolian samples are low. This indicates a dearth of first cycle volcanogenic zircons and points to minimal contribution of direct ashfall detritus to the Pampean eolian system relative to the total volume of sediment. Although initially surprising, these results are consistent with the regional volcanic history. The proportions of <23 Ma in the eolian samples are generally greater than the $N = 3$ fluvial samples. That indicates: (*i*) a notable contribution from the Andean Cordillera, specifically volcanic rocks therein, and also suggests (*ii*) if the majority of detritus in the late Pleistocene Pampean eolian system was deflated from the ríos Desaguadero, Colorado, and/or Negro floodplains an additional source of Neogene zircons was probably involved. This could indicate direct eolian contribution of detritus from late Cenozoic volcanic rocks of the Cordillera as generally supported by the petrology of those sediments and sedimentary rocks (Fig. 6). More precisely locating the source area of these Neogene zircon crystals with the Cordillera may (a) clarify the sediment transport pathway taken by this portion of sediment to the Pampean eolian system, and (b) inform on synoptic winds during transport.

(2) Loessic sediments exposed along the Atlantic coast of the Pampa region (near Mar del Plata) indicate at least two distinct provenance signatures; one provenance signature is more closely associated with the lower Río Colorado and Río Negro lacking Neogene detrital zircons (19AR17), whereas the other shows similarity to the detrital zircon age signature of loess and eolian dune samples from the central

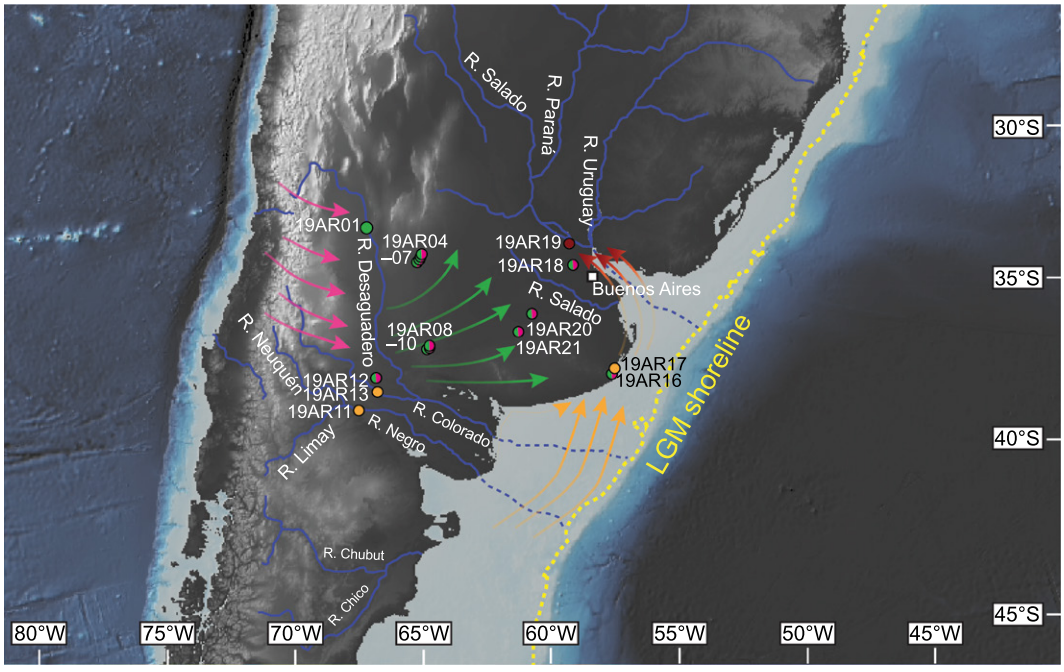

Figure 6. Summary of provenance interpretations based on U-Pb detrital zircon data presented herein and previously published fluvial and bedrock samples from southern South America. Simplified Last Glacial Maximum (LGM) shoreline from Guilderson et al. (2000). Magenta arrows: Andean Cordilleran source of detrital zircons, including Miocene and younger detrital zircons. Green arrows: deflation of Río Desaguadero floodplain (and possibly Río Colorado and Río Negro). Orange arrows: deflation of the subaerially exposed continental shelf during marine low stand and longshore transport. Red arrows: possible pathway of eolian sediments deflated from the subaerially exposed Río Paraná delta. Filled dots represent sample locations and simplified provenance scenarios—colors associated with arrows.

and northwestern Pampa (19AR16). Knowing the depositional age of these units will be important for differentiating between hypotheses. We speculate that one unit was largely derived through deflation of the lower Río Colorado and Río Negro floodplains during a low-stand in sea-level (e.g., Zárate and Blasi, 1993) or perhaps through longshore transport (e.g., Garzanti et al., 2021b), whereas the other unit was derived through a sediment transport pathway similar to samples in central Pampa (Fig. 6).

(3) A loess sampled from near the Argentine Río Paraná delta plain yielded a provenance signature much different than other samples within the Pampean eolian system. This sample yielded a provenance signature more closely associated with the Río Paraná rather than the ríos Deseguadero, Colorado, and/or Negro like most of the Pampean samples. From this we infer that these sediments were derived from greater exposure of the Río Paraná delta on the continental shelf during a low-stand in sea-level implying approximately northwestward eolian transport. That scenario fits with the known range in depositional age for the sample (i.e., 14.4–27.8 ka). Alternatively, the sediment may have been even more locally derived from the portion of the proximal delta plain that is currently exposed subaerially. The former scenario would hint at some consistency of lower-level winds which indicate an anticlockwise rotation through the Pampa during late Pleistocene to early Holocene from the surface expression of widespread linear erosional features impounded by shallow lakes (Fig. 6; Fucks et al., 2012). Identifying additional provenance variations for loessic sediments—especially across time, in this area like those now recognized for the Mar del Plata area coupled with depositional ages—would be informative in the understanding of the complexities of the Pampean eolian system under changing regional (and global) climate conditions.

ACKNOWLEDGMENTS

This research was funded by the U.S. National Science Foundation (EAR1946496 and EAR1910510). Jubal Sexton provided assistance in laser ablation–inductively coupled plasma–mass spectrometry data acquisition at the Center for Elemental Mass Spectrometry at the University of South Carolina, USA. We thank Francisco Juan Prevosti for his logistical assistance, collaboration, and friendship. This manuscript was improved by comments from an anonymous reviewer. Thanks to T. Capaldi for his review and all of his suggestions and helpful comments.

REFERENCES CITED

Abell, J.T., Winckler, G., Anderson, R.F., and Herbert, T.D., 2021, Poleward and weakened westerlies during Pliocene warmth: Nature, v. 589, 7840, p. 70–75, https://doi.org/10.1038/s41586-020-03062-1.

Abelmann, A., Gersonde, R., Cortese, G., Kuhn, G., and Smetacek, V., 2006, Extensive phytoplankton blooms in the Atlantic sector of the glacial Southern Ocean: Paleoceanography and Paleoclimatology, v. 21, no. 1, PA1013, https://doi.org/10.1029/2005PA001199.

Adams, C., Miller, H., Aceñolaza, F., Toselli, A., and Griffin, W., 2011, The Pacific Gondwana margin in the late Neoproterozoic–early Paleozoic: Detrital zircon U-Pb ages from metasediments in northwest Argentina reveal their maximum age, provenance and tectonic setting: Gondwana Research, v. 19, no. 1, p. 71–83, https://doi.org/10.1016/j.gr.2010.05.002.

Albani, S., Mahowald, N., Murphy, L., Raiswell, R., Moore, J., Anderson, R., McGee, D., Bradtmiller, L., Delmonte, B., and Hesse, P., 2016, Paleodust variability since the Last Glacial Maximum and implications for iron inputs to the ocean: Geophysical Research Letters, v. 43, no. 8, p. 3944–3954, https://doi.org/10.1002/2016GL067911.

Aliaga, V.S., Ferrelli, F., and Piccolo, M.C., 2017, Regionalization of climate over the Argentine Pampas: International Journal of Climatology, v. 37, p. 1237–1247, https://doi.org/10.1002/joc.5079.

Amidon, W.H., Ciccioli, P.L., Marenssi, S.A., Limarino, C.O., Fisher, G.B., Burbank, D.W., and Kylander-Clark, A., 2016, U-Pb ages of detrital and volcanic zircons of the Toro Negro Formation, northwestern Argentina: Age, provenance and sedimentation rates: Journal of South American Earth Sciences, v. 70, p. 237–250, https://doi.org/10.1016/j.jsames.2016.05.013.

Amit, R., Enzel, Y., Crouvi, O., Simhai, O., Matmon, A., Porat, N., McDonald, E., and Gillespie, A.R., 2011, The role of the Nile in initiating a massive dust influx to the Negev late in the middle Pleistocene: Geological Society of America Bulletin, v. 123, no. 5–6, p. 873–889, https://doi.org/10.1130/B30241.1.

Amsler, M.L., Drago, E.C., and Paira, A.R., 2007, Fluvial sediments: Main channel and floodplain interrelationships, *in* Iriondo, M.H., Paggi, J.C., and Parma, M.J., eds., The Middle Paraná River: Limnology of a Subtropical Wetland: Berlin, Germany, Springer, p. 123–142.

Anderson, R., Ali, S., Bradtmiller, L., Nielsen, S., Fleisher, M., Anderson, B., and Burckle, L., 2009, Wind-driven upwelling in the Southern Ocean and the deglacial rise in atmospheric CO_2: Science, v. 323, no. 5920, p. 1443–1448, http://doi.org/10.1126/science.1167441.

Anderson, R.F., Barker, S., Fleisher, M., Gersonde, R., Goldstein, S.L., Kuhn, G., Mortyn, P. G., Pahnke, K., and Sachs, J.P., 2014, Biological response to millennial variability of dust and nutrient supply in the Subantarctic South Atlantic Ocean: Philosophical Transactions of the Royal Society A: Mathematical, Physical and Engineering Sciences, v. 372, no. 2019, https://doi.org/10.1098/rsta.2013.0054.

Augustsson, C., Rusing, T., Adams, C.J., Chmiel, H., Kocabayoglu, M., Buld, M., Zimmermann, U., Berndt, J., and Kooijman, E., 2011, Detrital quartz and zircon combined: The production of mature sand with short transportation paths along the Cambrian West Gondwana margin, northwestern Argentina: Journal of Sedimentary Research, v. 81, p. 284–298, https://doi.org/10.2110/jsr.2011.23.

Bahlburg, H., Vervoort, J.D., Du Frane, S.A., Bock, B., Augustsson, C., and Reimann, C., 2009, Timing of crust formation and recycling in accretionary orogens: Insights learned from the western margin of South America: Earth-Science Reviews, v. 97, no. 1–4, p. 215–241, https://doi.org/10.1016/j.earscirev.2009.10.006.

Balgord, E.A., 2017, Triassic to Neogene evolution of the south-central Andean arc determined by detrital zircon U-Pb and Hf analysis of Neuquén Basin strata, central Argentina (34°S–40°S): Lithosphere, v. 9, no. 3, p. 453–462, https://doi.org/10.1130/L546.1.

Barbeau, D.L., Jr., Olivero, E.B., Swanson-Hysell, N.L., Zahid, K.M., Murray, K.E., and Gehrels, G.E., 2009, Detrital-zircon geochronology of the eastern Magallanes foreland basin: Implications for Eocene kinematics of the northern Scotia Arc and Drake Passage: Earth and Planetary Science Letters, v. 284, p. 489–503, https://doi.org/10.1016/j.epsl.2009.05.014.

Bastías-Mercado, F., González, J., and Oliveros, V., 2020, Volumetric and compositional estimation of the Choiyoi Magmatic Province and its comparison with other Silicic Large Igneous Provinces: Journal of South American Earth Sciences, v. 103, https://doi.org/10.1016/j.jsames.2020.102749.

Berman, A.L., Silvestri, G.E., and Tonello, M.S., 2016, Differences between Last Glacial Maximum and present-day temperature and precipitation in southern South America: Quaternary Science Reviews, v. 150, p. 221–233, https://doi.org/10.1016/j.quascirev.2016.08.025.

Bettis, E.A., III, Muhs, D.R., Roberts, H.M., and Wintle, A.G., 2003, Last glacial loess in the conterminous USA: Quaternary Science Reviews, v. 22, no. 18–19, p. 1907–1946, https://doi.org/10.1016/S0277-3791(03)00169-0.

Bird, A., Stevens, T., Rittner, M., Vermeesch, P., Carter, A., Andò, S., Garzanti, E., Lu, H., Nie, J., and Zeng, L., 2015, Quaternary dust source variation across the Chinese Loess Plateau: Palaeogeography, Palaeoclimatology, Palaeoecology, v. 435, p. 254–264, https://doi.org/10.1016/j.palaeo.2015.06.024.

Black, L.P., Kamo, S.L., Allen, C.M., Davis, D.W., Aleinikoff, J.N., Valley, J.W., Mundil, R., Campbell, I.H., Korsch, R.J., Williams, I.S., and Foudoulis, C., 2004, Improved $^{206}Pb/^{238}U$ microprobe geochronology by the monitoring of a trace-element-related matrix effect; SHRIMP, ID-TIMS, ELA-ICP-MS and oxygen isotope documentation for a series of zircon standards: Chemical Geology, v. 205, no. 1, p. 115–140, https://doi.org/10.1016/j.chemgeo.2004.01.003.

Boex, J., Fogwill, C., Harrison, S., Glasser, N., Hein, A., Schnabel, C., and Xu, S., 2013, Rapid thinning of the late Pleistocene Patagonian Ice Sheet followed migration of the Southern Westerlies: Scientific Reports, v. 3, no. 1, https://doi.org/10.1038/srep02118.

Bopp, L., Kohfeld, K.E., Le Quéré, C., and Aumont, O., 2003, Dust impact on marine biota and atmospheric CO_2 during glacial periods: Paleoceanography and Paleoclimatology, v. 18, no. 2, 1046, https://doi.org/10.1029/2002PA000810.

Boyd, P., and Law, C., 2001, The Southern Ocean iron release experiment (SOIREE): Introduction and summary: Deep-sea Research. Part II, Topical Studies in Oceanography, v. 48, no. 11–12, p. 2425–2438, https://doi.org/10.1016/S0967-0645(01)00002-9.

Capaldi, T.N., Horton, B.K., McKenzie, N.R., Stockli, D.F., and Odlum, M.L., 2017, Sediment provenance in contractional orogens: The detrital zircon record from modern rivers in the Andean fold-thrust belt and foreland basin of western Argentina: Earth and Planetary Science Letters, v. 479, p. 83–97, https://doi.org/10.1016/j.epsl.2017.09.001.

Capaldi, T.N., George, S.W.M., Hirtz, J.A., Horton, B.K., and Stockli, D.F., 2019, Fluvial and eolian sediment mixing during changing climate conditions recorded in Holocene Andean foreland deposits from Argentina (31–33°S): Frontiers of Earth Science, v. 7, https://doi.org/10.3389/feart.2019.00298.

Capaldi, T.N., McKenzie, N.R., Horton, B.K., Mackaman-Lofland, C., Colleps, C.L., and Stockli, D.F., 2021, Detrital zircon record of Phanerozoic magmatism in the southern Central Andes: Geosphere, v. 17, p. 876–897, https://doi.org/10.1130/GES02346.1.

Church, M.J., Hutchins, D.A., and Ducklow, H.W., 2000, Limitation of bacterial growth by dissolved organic matter and iron in the Southern Ocean: Applied and Environmental Microbiology, v. 66, no. 2, p. 455–466, https://doi.org/10.1128/AEM.66.2.455-466.2000.

Clapperton, C., 1993, Quaternary geology and geomorphology of South America: Amsterdam, Netherlands, Elsevier, 779 p.

Crouvi, O., Amit, R., Enzel, Y., Porat, N., and Sandler, A., 2008, Sand dunes as a major proximal dust source for late Pleistocene loess in the Negev Desert, Israel: Quaternary Research, v. 70, no. 2, p. 275–282, https://doi.org/10.1016/j.yqres.2008.04.011.

de Baar, H.J., De Jong, J.T., Bakker, D.C., Löscher, B.M., Veth, C., Bathmann, U., and Smetacek, V., 1995, Importance of iron for plankton blooms and carbon dioxide drawdown in the Southern Ocean: Nature, v. 373, no. 6513, p. 412–415, https://doi.org/10.1038/373412a0.

DeCelles, P.G., Carrapa, B., and Gehrels, G.E., 2007, Detrital zircon U-Pb ages provide provenance and chronostratigraphic information from Eocene synorogenic deposits in northwestern Argentina: Geology, v. 35, no. 4, p. 323–326, https://doi.org/10.1130/G23322A.1.

Delmonte, B., Paleari, C.I., Andò, S., Garzanti, E., Andersson, P.S., Petit, J.R., Crosta, X., Narcisi, B., Baroni, C., and Salvatore, M.C., 2017, Causes of dust size variability in central East Antarctica (Dome B): Atmospheric transport from expanded South American sources during Marine Isotope Stage 2: Quaternary Science Reviews, v. 168, p. 55–68, https://doi.org/10.1016/j.quascirev.2017.05.009.

Encinas, A., Pérez, F., Nielsen, S.N., Finger, K.L., Valencia, V., and Duhart, P., 2014, Geochronologic and paleontologic evidence for a Pacific–Atlantic connection during the late Oligocene–early Miocene in the Patagonian Andes (43–44°S): Journal of South American Earth Sciences, v. 55, p. 1–18, https://doi.org/10.1016/j.jsames.2014.06.008.

Enkelmann, E., Ridgway, K.D., Carignano, C., and Linnemann, U., 2014, A thermochronometric view into an ancient landscape: Tectonic setting, development, and inversion of the Paleozoic eastern Paganzo basin, Argentina: Lithosphere, v. 6, p. 93–107, https://doi.org/10.1130/L309.1.

Enzel, Y., Amit, R., Dayan, U., Crouvi, O., Kahana, R., Ziv, B., and Sharon, D., 2008, The climatic and physiographic controls of the eastern Mediterranean over the late Pleistocene climates in the southern Levant and its neighboring deserts: Global and Planetary Change, v. 60, no. 3–4, p. 165–192, https://doi.org/10.1016/j.gloplacha.2007.02.003.

Forman, S.L., Tripaldi, A., and Ciccioli, P.L., 2014, Eolian sand sheet deposition in the San Luis paleodune field, western Argentina as an indicator of a semi-arid environment through the Holocene: Palaeogeography, Palaeoclimatology, Palaeoecology, v. 411, p. 122–135, https://doi.org/10.1016/j.palaeo.2014.05.038.

Fosdick, J.C., Carrapa, B., and Ortiz, G., 2015, Faulting and erosion in the Argentine Precordillera during changes in subduction regime: Reconciling bedrock cooling and detrital records: Earth and Planetary Science Letters, v. 432, p. 73–83, https://doi.org/10.1016/j.epsl.2015.09.041.

Fosdick, J.C., Reat, E.J., Carrapa, B., Ortiz, G., and Alvarado, P.M., 2017, Retroarc basin reorganization and aridification during Paleogene uplift of the southern central Andes: Tectonics, v. 36, no. 3, p. 493–514, https://doi.org/10.1002/2016TC004400.

Fucks, E., Pisano, F., Carbonari, J., and Huarte, R., 2012, Aspectos geomorfológicos del sector medio e inferior de la Pampa Deprimida, provincia de Buenos Aires: Revista de la Sociedad Geológica de España, v. 25, no. 1–2.

Gaiero, D.M., 2007, Dust provenance in Antarctic ice during glacial periods: From where in southern South America?: Geophysical Research Letters, v. 34, no. 17, L17707, https://doi.org/10.1029/2007GL030520.

Gaiero, D.M., Probst, J.-L., Depetris, P.J., Bidart, S.M., and Leleyter, L., 2003, Iron and other transition metals in Patagonian riverborne and windborne materials: Geochemical control and transport to the southern South Atlantic Ocean: Geochimica et Cosmochimica Acta, v. 67, no. 19, p. 3603–3623, https://doi.org/10.1016/S0016-7037(03)00211-4.

Gaiero, D.M., Simonella, L., Gassó, S., Gili, S., Stein, A., Sosa, P., Becchio, R., Arce, J., and Marelli, H., 2013, Ground/satellite observations and atmospheric modeling of dust storms originating in the high Puna-Altiplano deserts (South America): Implications for the interpretation of paleo-climatic archives: Journal of Geophysical Research, D, Atmospheres, v. 118, no. 9, p. 3817–3831, https://doi.org/10.1002/jgrd.50036.

Garreaud, R.D., Vuille, M., Compagnucci, R., and Marengo, J., 2009, Present-day South American climate: Palaeogeography, Palaeoclimatology, Palaeoecology, v. 281, no. 3–4, p. 180–195, https://doi.org/10.1016/j.palaeo.2007.10.032.

Garzanti, E., Capaldi, T.N., Limonta, M., Sosa, N., and Vezzoli, G., 2021a, Transcontinental retroarc sediment routing controlled by subduction geometry and climate change (Central and Southern Andes, Argentina): Basin Research, v. 33, p. 3406–3437, https://doi.org/10.1111/bre.12607.

Garzanti, E., Limonta, M., Vezzoli, G., and Sosa, N., 2021b, From Patagonia to Río de la Plata: Multistep long-distance littoral transport of Andean volcaniclastic sand along the Argentine passive margin: Sedimentology, v. 68, p. 3357–3384, https://doi.org/10.1111/sed.12902.

Gehrels, G., Valencia, V., and Pullen, A., 2006, Detrital zircon geochronology by laser-ablation multicollector ICPMS at the Arizona LaserChron Center: The Paleontological Society Papers, v. 12, p. 67–76, https://doi.org/10.1017/S1089332600001352.

Gehrels, G.E., Valencia, V.A., and Ruiz, J., 2008, Enhanced precision, accuracy, efficiency, and spatial resolution of U-Pb ages by laser ablation–multicollector–inductively coupled plasma–mass spectrometry: Geochemistry, Geophysics, Geosystems, v. 9, no. 3, Q03017, https://doi.org/10.1029/2007GC001805.

Gili, S., Gaiero, D.M., Goldstein, S.L., Chemale, F., Jr., Koester, E., Jweda, J., Vallelonga, P., and Kaplan, M.R., 2016, Provenance of dust to Antarctica: A lead isotopic perspective: Geophysical Research Letters, v. 43, no. 5, p. 2291–2298, https://doi.org/10.1002/2016GL068244.

Gili, S., Gaiero, D.M., Goldstein, S.L., Chemale, F., Jr., Jweda, J., Kaplan, M.R., Becchio, R.A., and Koester, E., 2017, Glacial/interglacial changes of Southern Hemisphere wind circulation from the geochemistry of South American dust: Earth and Planetary Science Letters, v. 469, p. 98–109, https://doi.org/10.1016/j.epsl.2017.04.007.

Gómez, J., Schobbenhous, C., and Montes, N.E., 2019, Geological Map of South America: Commission for the Geological Map of the World, Columbian Geological Survey and the Geological Survey of Brazil, scale 1:5,000,000.

González Bonorino, F., 1965, Mineralogia de las franciones arcilla y limo del Pampeano en el area de la Ciudad de Buenos Aires y su significado estratigrafico y sedimentoligico: Revista de la Asociación Geológica Argentina, v. 20, p. 67–148.

Grimley, D.A., 2000, Glacial and nonglacial sediment contributions to Wisconsin Episode loess in the central United States: Geological Society of America Bulletin, v. 112, no. 10, p. 1475–1495, https://doi.org/10.1130/0016-7606(2000)112<1475:GANSCT>2.0.CO;2.

Grousset, F.E., Biscaye, P.E., Revel, M., Petit, J.-R., Pye, K., Joussaume, S., and Jouzel, J., 1992, Antarctic (Dome C) ice-core dust at 18 ky BP: Isotopic constraints on origins: Earth and Planetary Science Letters, v. 111, no. 1, p. 175–182, https://doi.org/10.1016/0012-821X(92)90177-W.

Guilderson, T., Burckle, L., Hemming, S., and Peltier, W., 2000, Late Pleistocene sea level variations derived from the Argentine Shelf: Geochemistry, Geophysics, Geosystems, v. 1, no. 12, https://doi.org/10.1029/2000GC000098.

Hansen, J., and Nazarenko, L., 2004, Soot climate forcing via snow and ice albedos: Proceedings of the National Academy of Sciences of the United States of America, v. 101, no. 2, p. 423–428, https://doi.org/10.1073/pnas.2237157100.

Henríquez, S., DeCelles, P.G., and Carrapa, B., 2019, Cretaceous to middle Cenozoic exhumation history of the Cordillera de Domeyko and Salar de Atacama basin, northern Chile: Tectonics, v. 38, no. 2, p. 395–416, https://doi.org/10.1029/2018TC005203.

Henríquez, S.D.P., Carrapa, B., Hughes, A.N., Davis, G.H., and Alvarado, P., 2020, Deformation history of the Puna plateau, Central Andes of northwestern Argentina: Journal of Structural Geology, v. 140, https://doi.org/10.1016/j.jsg.2020.104133.

Hervé, F., Fanning, C.M., and Pankhurst, R.J., 2003, Detrital zircon age patterns and provenance of the metamorphic complexes of southern Chile: Journal of South American Earth Sciences, v. 16, p. 107–123, https://doi.org/10.1016/S0895-9811(03)00022-1.

Hoke, G.D., Schmitz, M.D., and Bowring, S.A., 2014, An ultrasonic method for isolating nonclay components from clay-rich material: Geochemistry, Geophysics, Geosystems, v. 15, no. 2, p. 492–498, https://doi.org/10.1002/2013GC005125.

Huang, J., Minnis, P., Lin, B., Wang, T., Yi, Y., Hu, Y., Sun-Mack, S., and Ayers, K., 2006, Possible influences of Asian dust aerosols on cloud properties and radiative forcing observed from MODIS and CERES: Geophysical Research Letters, v. 33, no. 6, L06824, https://doi.org/10.1029/2005GL024724.

Ibañez-Mejia, M., Pullen, A., Pepper, M., Urbani, F., Ghoshal, G., and Ibañez-Mejia, J.C., 2018, Use and abuse of detrital zircon U-Pb geochronology: A case from the Río Orinoco delta, eastern Venezuela: Geology, v. 46, p. 1019–1022, https://doi.org/10.1130/G45596.1.

Imbellone, P.A., and Teruggi, M.E., 1993, Paleosols in loess deposits of the Argentine Pampas: Quaternary International, v. 17, p. 49–55, https://doi.org/10.1016/1040-6182(93)90080-Y.

Iriondo, M., 1990, Map of the South American Plains: Its present state, *in* Rabassa, J., ed., Quaternary of South America and Antarctic Peninsula: London, UK, CRC Press, map 12 p.

Iriondo, M.H., 1997, Models of deposition of loess and loessoids in the upper Quaternary of South America: Journal of South American Earth Sciences, v. 10, no. 1, p. 71–79, https://doi.org/10.1016/S0895-9811(97)00006-0.

Iriondo, M.N., 1999, The origin of silt particles in the loess question: Quaternary International, v. 62, no. 1, p. 3–9, https://doi.org/10.1016/S1040-6182(99)00018-X.

Iriondo, M.H., and García, N.O., 1993, Climatic variations in the Argentine plains during the last 18,000 years: Palaeogeography, Palaeoclimatology, Palaeoecology, v. 101, no. 3–4, p. 209–220, https://doi.org/10.1016/0031-0182(93)90013-9.

Iriondo, M.H., and Kröhling, D.M., 2007, Non-classical types of loess: Sedimentary Geology, v. 202, p. 352–368, https://doi.org/10.1016/j.sedgeo.2007.03.012.

Iriondo, M., Brunetto, E., and Kröhling, D., 2009, Historical climatic extremes as indicators for typical scenarios of Holocene climatic periods in the Pampean plain: Palaeogeography, Palaeoclimatology, Palaeoecology, v. 283, no. 3–4, p. 107–119, https://doi.org/10.1016/j.palaeo.2009.09.005.

Jickells, T., An, Z., Andersen, K. K., Baker, A., Bergametti, G., Brooks, N., Cao, J., Boyd, P., Duce, R., and Hunter, K., 2005, Global iron connections between desert dust, ocean biogeochemistry, and climate: Science, v. 308, p. 67–71, https://doi.org/10.1126/science.1105959.

Johnson, M., Meskhidze, N., Kiliyanpilakkil, V., and Gassó, S., 2011, Understanding the transport of Patagonian dust and its influence on marine biological activity in the South Atlantic Ocean: Atmospheric Chemistry and Physics, v. 11, no. 6, p. 2487–2502, https://doi.org/10.5194/acp-11-2487-2011.

Kemp, R., Toms, P., King, M., and Kröhling, D., 2004, The pedosedimentary evolution and chronology of Tortugas, a Late Quaternary type-site of the northern Pampa, Argentina: Quaternary International, v. 114, no. 1, p. 101–112, https://doi.org/10.1016/S1040-6182(03)00045-4.

Kemp, R.A., Zárate, M., Toms, P., King, M., Sanabria, J., and Arguello, G., 2006, Late Quaternary paleosols, stratigraphy and landscape evolution in the Northern Pampa, Argentina: Quaternary Research, v. 66, no. 1, p. 119–132, https://doi.org/10.1016/j.yqres.2006.01.001.

Kohfeld, K., Graham, R., De Boer, A., Sime, L., Wolff, E., Le Quéré, C., and Bopp, L., 2013, Southern Hemisphere westerly wind changes during the Last Glacial Maximum: paleo-data synthesis: Quaternary Science Reviews, v. 68, p. 76–95, https://doi.org/10.1016/j.quascirev.2013.01.017.

Krinitzsky, E.L., and Turnbull, W.J., 1967, Loess deposits of Mississippi: Geological Society of America Special Paper 94, 64 p., https://doi.org/10.1130/SPE94-p1.

Kröhling, D.M., 1999, Sedimentological maps of the typical loessic units in North Pampa, Argentina: Quaternary International, v. 62, no. 1, p. 49–55, https://doi.org/10.1016/S1040-6182(99)00022-1.

Kruck, W., Helms, F., Geyh, M.A., Suriano, J.M., Marengo, H.G., and Pereyra, F., 2011, Late Pleistocene-Holocene history of Chaco-Pampa sediments in Argentina and Paraguay: E&G Quaternary Science Journal, v. 60, p. 188–202, https://doi.org/10.3285/eg.60.1.13.

Kumar, P., Sokolik, I., and Nenes, A., 2011, Measurements of cloud condensation nuclei activity and droplet activation kinetics of fresh unprocessed regional dust samples and minerals: Atmospheric Chemistry and Physics, v. 11, no. 7, p. 3527–3541, https://doi.org/10.5194/acp-11-3527-2011.

Leonard, J.S., Fosdick, J.C., and VanderLeest, R.A., 2020, Erosional and tectonic evolution of a retroarc orogenic

wedge as revealed by sedimentary provenance: Case of the Oligocene–Miocene Patagonian Andes: Frontiers of Earth Science, v. 7, https://doi.org/10.3389/feart.2019.00353.

Luppo, T., de Luchi, M.G.L., Rapalini, A.E., Dopico, C.I.M., and Fanning, C.M., 2018, Geochronologic evidence of a large magmatic province in northern Patagonia encompassing the Permian-Triassic boundary: Journal of South American Earth Sciences, v. 82, p. 346–355, https://doi.org/10.1016/j.jsames.2018.01.003.

Lyell, C., 1834, Observations on the loamy deposit called 'loess' in the valley of the Rhine: Proceedings of the Geological Society of London, v. 2, p. 21–22.

Maher, B., Prospero, J., Mackie, D., Gaiero, D., Hesse, P.P., and Balkanski, Y., 2010, Global connections between aeolian dust, climate and ocean biogeochemistry at the present day and at the last glacial maximum: Earth-Science Reviews, v. 99, no. 1–2, p. 61–97, https://doi.org/10.1016/j.earscirev.2009.12.001.

Martin, J.H., Gordon, R.M., and Fitzwater, S.E., 1990, Iron in Antarctic waters: Nature, v. 345, p. 156–158, https://doi.org/10.1038/345156a0.

Martínez-Garcia, A., Rosell-Melé, A., Jaccard, S.L., Geibert, W., Sigman, D.M., and Haug, G.H., 2011, Southern Ocean dust–climate coupling over the past four million years: Nature, v. 476, no. 7360, p. 312–315, https://doi.org/10.1038/nature10310.

Martini, M.A., Kaplan, M.R., Strelin, J.A., Astini, R.A., Schaefer, J.M., Caffee, M.W., and Schwartz, R., 2017, Late Pleistocene glacial fluctuations in Cordillera oriental, subtropical Andes: Quaternary Science Reviews, v. 171, p. 245–259, https://doi.org/10.1016/j.quascirev.2017.06.033.

Mattinson, J.M., 2010, Analysis of the relative decay constants of ^{235}U and ^{238}U by multi-step CA-TIMS measurements of closed-system natural zircon samples: Chemical Geology, v. 275, no. 3, p. 186–198, https://doi.org/10.1016/j.chemgeo.2010.05.007.

McGlue, M.M., Smith, P.H., Zani, H., Silva, A., Carrapa, B., Cohen, A.S., and Pepper, M.B., 2016, An integrated sedimentary systems analysis of the Río Bermejo (Argentina): Megafan character in the overfilled Southern Chaco foreland basin: Journal of Sedimentary Research, v. 86, no. 12, p. 1359–1377, https://doi.org/10.2110/jsr.2016.82.

McMillan, M., and Schoenbohm, L.M., 2020, Large-scale Cenozoic wind erosion in the Puna Plateau: The Salina del Fraile Depression: Journal of Geophysical Research: Earth Surface, v. 125, no. 9, https://doi.org/10.1029/2020JF005682.

Milana, J.P., and Kröhling, D.M., 2017, First data on volume and type of deflated sediment from Southern Puna Plateau and its role as source of the Chaco-Pampean loess, *in* Kröhling, D.M., ed., Analysis of the Quaternary Climatic and Tectonic Forcing Along Some Different Tectonic Settings of South America: Quaternary International, v. 438, p. 126–140, https://doi.org/10.1016/j.quaint.2017.03.007.

Miller, R.L., Knippertz, P., García-Pando, C.P., Perlwitz, J.P., and Tegen, I., 2014, Impact of dust radiative forcing upon climate, *in* Knippertz, P., and Stuut, J-.B.W., eds., Mineral Dust: A Key Player in the Earth System: Berlin, Germany, Springer, p. 327–357, https://doi.org/10.1007/978-94-017-8978-3_13.

Moore, C., Mills, M., Arrigo, K., Berman-Frank, I., Bopp, L., Boyd, P., Galbraith, E., Geider, R., Guieu, C., and Jaccard, S., 2013, Processes and patterns of oceanic nutrient limitation: Nature Geoscience, v. 6, p. 701–710, https://doi.org/10.1038/ngeo1765.

Morosini, A.F., Suárez, A.E.O., Otamendi, J.E., Pagano, D.S., and Ramos, G.A., 2017, La Escalerilla pluton, San Luis Argentina: The orogenic and post-orogenic magmatic evolution of the Famatinian cycle at Sierras de San Luis: Journal of South American Earth Sciences, v. 73, p. 100–118, https://doi.org/10.1016/j.jsames.2016.12.001.

Morrás, H., 1997, Origen y mineralogía del material parental de los suelos de la región Pampeana: Homogeneidad o Heterogeneidad, v. 1, p. 19–20.

Mpodozis, C., and Kay, S.M., 1992, Late Paleozoic to Triassic evolution of the Gondwana margin: Evidence from Chilean Frontal Cordilleran batholiths (28°S to 31°S): Geological Society of America Bulletin, v. 104, no. 8, p. 999–1014, https://doi.org/10.1130/0016-7606(1992)104<0999:LPTTEO>2.3.CO;2.

Muhs, D.R., 2007, Loess deposits, origins and properties, *in* Elias, S.A., ed., Encyclopedia of Quaternary Science: Amsterdam, Netherlands, Elsevier, p. 1405–1418, https://doi.org/10.1016/B0-44-452747-8/00158-7.

Muhs, D.R., 2013, The geologic records of dust in the Quaternary: Aeolian Research, v. 9, p. 3–48, https://doi.org/10.1016/j.aeolia.2012.08.001.

Naipauer, M., Tapia, F., Mescua, J., Farías, M., Pimentel, M.M., and Ramos, V.A., 2015, Detrital and volcanic zircon U-Pb ages from southern Mendoza (Argentina): An insight on the source regions in the northern part of the Neuquén Basin: Journal of South American Earth Sciences, v. 64, p. 434–451, https://doi.org/10.1016/j.jsames.2015.09.013.

Nie, J., Stevens, T., Rittner, M., Stockli, D., Garzanti, E., Limonta, M., Bird, A., Ando, S., Vermeesch, P., and Saylor, J., 2015, Loess plateau storage of northeastern Tibetan plateau-derived Yellow River sediment: Nature Communications, v. 6, 8511, https://doi.org/10.1038/ncomms9511.

Obruchev, V., 1911, The question of the origin of loess in defense of the aeolian hypothesis: Izvêstiya Tomskago Tekhnologiceskago Instituta, v. 33.

Obruchev, V.A., 1945, Loess types and their origin: American Journal of Science, v. 243, no. 5, p. 256–262, https://doi.org/10.2475/ajs.243.5.256.

Otamendi, J.E., Cristofolini, E.A., Morosini, A., Armas, P., Tibaldi, A.M., and Camilletti, G.C., 2020, The geodynamic history of the Famatinian arc, Argentina: A record of exposed geology over the type section (latitudes 27°-33° south): Journal of South American Earth Sciences, v. 100, https://doi.org/10.1016/j.jsames.2020.102558.

Paces, J.B., and Miller, J.D., 1993, Precise U-Pb ages of Duluth Complex and related mafic intrusions, northeastern Minnesota: Geochronological insights to physical, petrogenetic, paleomagnetic, and tectonomagmatic processes associated with the 1.1 Ga Midcontinent Rift System: Journal of Geophysical Research. Solid Earth, v. 98, no. B8, p. 13,997–14,013, https://doi.org/10.1029/93JB01159.

Painter, T.H., Barrett, A.P., Landry, C.C., Neff, J.C., Cassidy, M.P., Lawrence, C.R., McBride, K.E., and Farmer, G.L., 2007, Impact of disturbed desert soils on duration of mountain snow cover: Geophysical Research Letters, v. 34, no. 12, L12502, https://doi.org/10.1029/2007GL030284.

Panario, D., and Gutiérrez, O., 1999, The continental Uruguayan Cenozoic: An overview: Quaternary International, v. 62, no. 1, p. 75–84, https://doi.org/10.1016/S1040-6182(99)00025-7.

Pankhurst, R.J., Rapela, C.W., Saavedra, J., Baldo, E., Dahlquist, J., Pascua, I., and Fanning, C.M., 1998, The Famatinian magmatic arc in the central Sierras Pampeanas: An Early to Mid-Ordovician continental arc on the Gondwana margin, *in* Pankhurst, R.J., and Rapela, C.W., eds., The Proto-Andean Margin of Gondwana: Geological Society of London, Special Publications, v. 142, p. 343–367, https://doi.org/10.1144/GSL.SP.1998.142.01.17.

Paparazzo, F.E., Crespi-Abril, A.C., Gonçalves, R.J., Barbieri, E.S., Villalobos, L.L.G., Solís, M.E., and Soria, G., 2018, Patagonian dust as a source of macronutrients in the Southwest Atlantic Ocean: Oceanography (Washington, D.C.), v. 31, no. 4, p. 33–39, https://doi.org/10.5670/oceanog.2018.408.

Pepper, M., Gehrels, G., Pullen, A., Ibañez-Mejia, M., Ward, K.M., and Kapp, P., 2016, Magmatic history and crustal genesis of western South America: Constraints from U-Pb ages and Hf isotopes of detrital zircons in modern rivers: Geosphere, v. 12, no. 5, p. 1532–1555, https://doi.org/10.1130/GES01315.1.

Prieto, A.R., 1996, Late Quaternary vegetational and climatic changes in the Pampa grassland of Argentina: Quaternary Research, v. 45, no. 1, p. 73–88, https://doi.org/10.1006/qres.1996.0007.

Pullen, A., Ibáñez-Mejía, M., Gehrels, G.E., Ibáñez-Mejía, J.C., and Pecha, M., 2014, What happens when n= 1000? Creating large-n geochronological datasets with LA-ICP-MS for geologic investigations: Journal of Analytical Atomic Spectrometry, v. 29, no. 6, p. 971–980, https://doi.org/10.1039/C4JA00024B.

Pullen, A., Ibáñez-Mejia, M., Gehrels, G. E., Giesler, D., and Pecha, M., 2018, Optimization of a laser ablation-single collector-inductively coupled plasma-mass spectrometer (Thermo Element 2) for accurate, precise, and efficient zircon U-Th-Pb geochronology: Geochemistry, Geophysics, Geosystems, v. 19, p. 3689–3705, https://doi.org/10.1029/2018GC007889.

Pye, K., 1995, The nature, origin and accumulation of loess: Quaternary Science Reviews, v. 14, no. 7–8, p. 653–667, https://doi.org/10.1016/0277-3791(95)00047-X.

Rabassa, J., Coronato, A.M., and Salemme, M., 2005, Chronology of the Late Cenozoic Patagonian glaciations and their correlation with biostratigraphic units of the Pampean region (Argentina): Journal of South American Earth Sciences, v. 20, no. 1–2, p. 81–103, https://doi.org/10.1016/j.jsames.2005.07.004.

Ramos, V.A., Zapata, T., Cristallini, E., and Introcaso, A., 2004, The Andean thrust system: Latitudinal variations in structural styles and orogenic shortening, *in* McClay, K.R., ed., Thrust Tectonics and Hydrocarbon Systems: AAPG Memoir 82, p. 30–50.

Ramos, V.A., 2009, Anatomy and global context of the Andes: Main geologic features and the Andean orogenic cycle, *in* Kay, S.M., Ramos, V.A., and Dickinson, W.R., eds., Backbone of the Americas: Shallow Subduction, Plateau Uplift, and Ridge and Terrane Collision: Geological Society of America Memoir 204, p. 31–65, https://doi.org/10.1130/2009.1204(02).

Ramos, V.A., and Folguera, A., 2009, Andean flat-slab subduction through time, *in* Murphy, J.B., Keppie, J.D., and Hynes, A.J., eds., Ancient Orogens and Modern Analogues: Geological Society of London Special Publication 327, p. 31–54.

Ramos, V.A., and Folguera, A., 2011, Payenia volcanic province in the Southern Andes: An appraisal of an exceptional Quaternary tectonic setting: Journal of Volcanology and Geothermal Research, v. 201, p. 53–64, https://doi.org/10.1016/j.jvolgeores.2010.09.008.

Ramos, V.A., Chemale, F., Naipauer, M., and Pazos, P.J., 2014, A provenance study of the Paleozoic Ventania System (Argentina): Transient complex sources from Western and Eastern Gondwana: Gondwana Research, v. 26, no. 2, p. 719–740, https://doi.org/10.1016/j.gr.2013.07.008.

Rapela, C.W., Verdecchia, S.O., Casquet, C., Pankhurst, R.J., Baldo, E.G., Galindo, C., Murra, J.A., Dahlquist, J.A., and Fanning, C.M., 2016, Identifying Laurentian and SW Gondwana sources in the Neoproterozoic to Early Paleozoic metasedimentary rocks of the Sierras Pampeanas: Paleogeographic and tectonic implications: Gondwana Research, v. 32, p. 193–212, https://doi.org/10.1016/j.gr.2015.02.010.

Reat, E.J., and Fosdick, J.C., 2018, Basin evolution during Cretaceous-Oligocene changes in sediment routing in the Eastern Precordillera, Argentina: Journal of South American Earth Sciences, v. 84, p. 422–443, https://doi.org/10.1016/j.jsames.2018.02.010.

Revel-Rolland, M., De Deckker, P., Delmonte, B., Hesse, P., Magee, J., Basile-Doelsch, I., Grousset, F., and Bosch, D., 2006, Eastern Australia: A possible source of dust in East Antarctica interglacial ice: Earth and Planetary Science Letters, v. 249, no. 1–2, p. 1–13, https://doi.org/10.1016/j.epsl.2006.06.028.

Richthofen, B.F., 1882, II. On the mode of origin of the loess: Geological Magazine, v. 9, no. 7, p. 293–305, https://doi.org/10.1017/S001675680017164X.

Ridgwell, A., and Watson, A.J., 2002, Feedback between aeolian dust, climate, and atmospheric CO_2 in glacial time: Paleooceanography and Paleoceanography, v. 17, no. 4, 1059, https://doi.org/10.1029/2001PA000729.

Rino, S., Kon, Y., Sato, W., Maruyama, S., Santosh, M., and Zhao, D., 2008, The Grenvillian and Pan-African orogens: World's largest orogenies through geologic time, and their implications on the origin of superplume: Gondwana Research, v. 14, p. 51–72, https://doi.org/10.1016/j.gr.2008.01.001.

Rocha-Campos, A.C., Basei, M.A., Nutman, A.P., Kleiman, L.E., Varela, R., Llambias, E., Canile, F.M., and Da Rosa, O.D.C., 2011, 30 million years of Permian

volcanism recorded in the Choiyoi igneous province (W Argentina) and their source for younger ash fall deposits in the Paraná Basin: SHRIMP U-Pb zircon geochronology evidence: Gondwana Research, v. 19, p. 509–523, https://doi.org/10.1016/j.gr.2010.07.003.

Russell, R.J., 1944, Lower Mississippi valley loess: Geological Society of America Bulletin, v. 55, no. 1, p. 1–40, https://doi.org/10.1130/GSAB-55-1.

Sato, A.M., Llambías, E.J., Basei, M.A., and Castro, C.E., 2015, Three stages in the Late Paleozoic to Triassic magmatism of southwestern Gondwana, and the relationships with the volcanogenic events in coeval basins: Journal of South American Earth Sciences, v. 63, p. 48–69, https://doi.org/10.1016/j.jsames.2015.07.005.

Sayago, J., Collantes, M., Karlson, A., and Sanabria, J., 2001, Genesis and distribution of the Late Pleistocene and Holocene loess of Argentina: A regional approximation: Quaternary International, v. 76, p. 247–257, https://doi.org/10.1016/S1040-6182(00)00107-5.

Scanza, R., Mahowald, N., Ghan, S., Zender, C., Kok, J., Liu, X., Zhang, Y., and Albani, S., 2015, Modeling dust as component minerals in the Community Atmosphere Model: Development of framework and impact on radiative forcing: Atmospheric Chemistry and Physics, v. 15, no. 1, p. 537–561, https://doi.org/10.5194/acp-15-537-2015.

Schwartz, J.J., Gromet, L.P., and Miro, R., 2008, Timing and duration of the calc-alkaline arc of the Pampean orogeny: Implications for the late Neoproterozoic to Cambrian evolution of western Gondwana: The Journal of Geology, v. 116, p. 39–61, https://doi.org/10.1086/524122.

Shoenfelt, E.M., Winckler, G., Lamy, F., Anderson, R.F., and Bostick, B.C., 2018, Highly bioavailable dustborne iron delivered to the Southern Ocean during glacial periods: Proceedings of the National Academy of Sciences of the United States of America, v. 115, no. 44, p. 11,180–11,185, https://doi.org/10.1073/pnas.1809755115.

Siks, B.C., and Horton, B.K., 2011, Growth and fragmentation of the Andean foreland basin during eastward advance of fold-thrust deformation, Puna plateau and Eastern Cordillera, northern Argentina: Tectonics, v. 30, no. 6, TC6017, https://doi.org/10.1029/2011TC002944.

Sláma, J., and Košler, J., 2012, Effects of sampling and mineral separation on accuracy of detrital zircon studies: Geochemistry Geophysics Geosystems, v. 13, no. 5, Q05007, https://doi.org/10.1029/2012GC004106.

Smalley, I., 1995, Making the material: The formation of silt sized primary mineral particles for loess deposits: Quaternary Science Reviews, v. 14, no. 7–8, p. 645–651, https://doi.org/10.1016/0277-3791(95)00046-1.

Smalley, I., O'Hara-Dhand, K., Wint, J., Machalett, B., Jary, Z., and Jefferson, I., 2009, Rivers and loess: the significance of long river transportation in the complex event-sequence approach to loess deposit formation: Quaternary International, v. 198, no. 1–2, p. 7–18, https://doi.org/10.1016/j.quaint.2008.06.009.

Smith, J., Vance, D., Kemp, R.A., Archer, C., Toms, P., King, M., and Zárate, M., 2003, Isotopic constraints on the source of Argentinian loess: With implications for atmospheric circulation and the provenance of Antarctic dust during recent glacial maxima: Earth and Planetary Science Letters, v. 212, no. 1–2, p. 181–196, https://doi.org/10.1016/S0012-821X(03)00260-7.

Sokolik, I.N., Winker, D., Bergametti, G., Gillette, D., Carmichael, G., Kaufman, Y., Gomes, L., Schuetz, L., and Penner, J., 2001, Introduction to special section: Outstanding problems in quantifying the radiative impacts of mineral dust: Journal of Geophysical Research, D, Atmospheres, v. 106, no. D16, p. 18,015–18,027, https://doi.org/10.1029/2000JD900498.

Stevens, T., Carter, A., Watson, T., Vermeesch, P., Andò, S., Bird, A., Lu, H., Garzanti, E., Cottam, M., and Sevastjanova, I., 2013, Genetic linkage between the Yellow River, the Mu Us desert and the Chinese loess plateau: Quaternary Science Reviews, v. 78, p. 355–368, https://doi.org/10.1016/j.quascirev.2012.11.032.

Streit, R.L., Burbank, D.W., Strecker, M.R., Alonso, R.N., Cottle, J.M., and Kylander-Clark, A.R., 2017, Controls on intermontane basin filling, isolation and incision on the margin of the Puna Plateau, NW Argentina (∼23°S): Basin Research, v. 29, p. 131–155, https://doi.org/10.1111/bre.12141.

Teruggi, M.E., 1957, The nature and origin of Argentine loess: Journal of Sedimentary Research, v. 27, no. 3, p. 322–332.

Thomas, W.A., Astini, R.A., Mueller, P.A., and McClelland, W.C., 2015, Detrital-zircon geochronology and provenance of the Ocloyic synorogenic clastic wedge, and Ordovician accretion of the Argentine Precordillera terrane: Geosphere, v. 11, p. 1749–1769, https://doi.org/10.1130/GES01212.1.

Toggweiler, J.R., and Russell, J., 2008, Ocean circulation in a warming climate: Nature, v. 451, p. 286–288, https://doi.org/10.1038/nature06590.

Tollo, R.P., Aleinikoff, J.N., Borduas, E.A., Hackley, P.C., and Fanning, C.M., 2004, Petrologic and geochronologic evolution of the Grenville orogen, northern Blue Ridge Province, Virginia, *in* Tollo, R.P., Corriveau, L., McLelland, J., and Bartholomew, M.J., eds., Proterozoic Tectonic Evolution of the Grenville Orogen in North America: Geological Society of America Memoir 197, p. 647–677, https://doi.org/10.1130/0-8137-1197-5.647.

Tripaldi, A., and Forman, S.L., 2007, Geomorphology and chronology of Late Quaternary dune fields of western Argentina: Palaeogeography, Palaeoclimatology, Palaeoecology, v. 251, p. 300–320, https://doi.org/10.1016/j.palaeo.2007.04.007.

Tripaldi, A., and Forman, S.L., 2016, Eolian depositional phases during the past 50 ka and inferred climate variability for the Pampean Sand Sea, western Pampas, Argentina: Quaternary Science Reviews, v. 139, p. 77–93, https://doi.org/10.1016/j.quascirev.2016.03.007.

Tripaldi, A., Zárate, M.A., Brook, G.A., and Li, G.-Q., 2011, Late Quaternary paleoenvironments and paleoclimatic conditions in the distal Andean piedmont, southern Mendoza, Argentina: Quaternary Research, v. 76, no. 2, p. 253–263, https://doi.org/10.1016/j.yqres.2011.06.008.

Tripaldi, A., Zárate, M.A., Forman, S.L., Badger, T., Doyle, M.E., and Ciccioli, P., 2013, Geological evidence for a drought episode in the western Pampas (Argentina, South America) during the early–mid 20th century: The Holocene, v. 23, no. 12, p. 1731–1746, https://doi.org/10.1177/0959683613505338.

Tripaldi, A., Mehl, A., and Zárate, M.A., 2018, Parabolic megadunes in a subtropical Quaternary inland dune field, southwestern Pampas, Argentina: Geomorphology, v. 321, p. 103–116, https://doi.org/10.1016/j.geomorph.2018.08.021.

Tsoar, H., and Pye, K., 1987, Dust transport and the question of desert loess formation: Sedimentology, v. 34, no. 1, p. 139–153, https://doi.org/10.1111/j.1365-3091.1987.tb00566.x.

Vanneste, H., De Vleeschouwer, F., Martínez-Cortizas, A., Von Scheffer, C., Piotrowska, N., Coronato, A., and Le Roux, G., 2015, Late-glacial elevated dust deposition linked to westerly wind shifts in southern South America: Scientific Reports, v. 5, no. 1, https://doi.org/10.1038/srep11670.

Violante, R.A., Paterlini, C., Marcolini, S., Costa, I., Cavallotto, J.L., Laprida, C., Dragani, W., Chapori, N.G., Watanabe, S., and Totah, V., 2014, The Argentine continental shelf: Morphology, sediments, processes and evolution since the Last Glacial Maximum: Geological Society, London, Memoir 41, no. 1, p. 55–68.

Wainer, I., Clauzet, G., Ledru, M.P., Brady, E., and Otto-Bliesner, B., 2005, Last Glacial Maximum in South America: Paleoclimate proxies and model results: Geophysical Research Letters, v. 32, no. 8, L08702, https://doi.org/10.1029/2004GL021244.

Zárate, M., and Blasi, A., 1993, Late Pleistocene-Holocene eolian deposits of the southern Buenos Aires Province, Argentina: A preliminary model: Quaternary International, v. 17, p. 15–20, https://doi.org/10.1016/1040-6182(93)90075-Q.

Zárate, M., Kemp, R., and Toms, P., 2009, Late Quaternary landscape reconstruction and geochronology in the northern Pampas of Buenos Aires province, Argentina: Journal of South American Earth Sciences, v. 27, no. 1, p. 88–99, https://doi.org/10.1016/j.jsames.2008.10.001.

Zárate, M.A., 2003, Loess of southern south America: Quaternary Science Reviews, v. 22, no. 18–19, p. 1987–2006, https://doi.org/10.1016/S0277-3791(03)00165-3.

Zárate, M.A., 2007, Loess records South America, *in* Elias, S.A., ed., Encyclopedia of Quaternary Science: London, UK, Elsevier, p. 1466–1479, https://doi.org/10.1016/B0-44-452747-8/00165-4.

Zárate, M.A., and Tripaldi, A., 2012, The aeolian system of central Argentina: Aeolian Research, v. 3, no. 4, p. 401–417, https://doi.org/10.1016/j.aeolia.2011.08.002.

Zhou, R., Schoenbohm, L.M., Sobel, E.R., Carrapa, B., and Davis, D.W., 2016, Sedimentary record of regional deformation and dynamics of the thick-skinned southern Puna Plateau, central Andes (26–27°S): Earth and Planetary Science Letters, v. 433, p. 317–325, https://doi.org/10.1016/j.epsl.2015.11.012.

Zhou, R., Schoenbohm, L.M., Sobel, E.R., Davis, D.W., and Glodny, J., 2017, New constraints on orogenic models of the southern Central Andean Plateau: Cenozoic basin evolution and bedrock exhumation: Geological Society of America Bulletin, v. 129, no. 1–2, p. 152–170, https://doi.org/10.1130/B31384.1.

Science Editor: Wenjiao Xiao
Associate Editor: William Guenthner

Manuscript Received 2 August 2021
Revised Manuscript Received 14 January 2022
Manuscript Accepted 15 March 2022

Printed in the USA